Summer 2019

The Dynamin-like Protein Vps1 Stimulates Endosome-to-Golgi Fusion in Vitro

Jared Christopher Smothers

Missouri State University, Smothers88@live.missouristate.edu

THE DYNAMIN-LIKE PROTEIN VPS1 STIMULATES ENDOSOME-TO-GOLGI

FUSION IN VITRO

A Master's Thesis

Presented to

The Graduate College of

Missouri State University

In Partial Fulfillment

Of the Requirements for the Degree

Master of Science, Biology

By

Jared C. Smothers

August 2019

THE DYNAMIN-LIKE PROTEIN VPS1 STIMULATES ENDOSOME-TO-GOLGI

FUSION IN VITRO

Biology

August 2019

Master of Science

Jared C. Smothers

ABSTRACT

Intracellular membrane fusion events can be reconstituted by exploiting isolated organelles from cellular hosts or artificial membranes made of purified phospholipid components. Artificial construction of membranes provides two significant advantages. First, cellular isolation of the endosome-derived vesicles and TGN (*trans*-Golgi Network) compartments needed for the fusion assay would be extremely challenging. Second, reconstituting the membranes provides the added benefit of controlling size and lipid compositions to functionally mimic the individual membrane architectures and introduce only the purified proteins that are under investigation. For these reasons, I have developed the first simultaneous lipid and content mixing fusion assays that measures the efficacy of endosome-to-TGN fusion and its promoted fusion capability with the dynamin-like protein Vps1 for the purposes of recapitulating the fusion. To quantify lipid mixing between the donor and recipient membrane fluorescent lipids (Rhodamine-PE and NBD-PE) were used, while content mixing was assessed by analyzing the increase of FRET between Cy5-streptavidin and PhycoE-biotin.

KEYWORDS: Vps1, Tlg2, endosome, TGN, membrane fusion, proteoliposome reconstitution, simultaneous fusion assay, lipid mixing, content mixing

THE DYNAMIN-LIKE PROTEIN VPS1 STIMULATES ENDOSOME-TO-GOLGI

FUSION IN VITRO

By

Jared C. Smothers

A Master's Thesis
Submitted to the Graduate College
Of Missouri State University
In Partial Fulfillment of the Requirements
For the Degree of Master of Science, Biology

August 2019

Kyoungtae Kim Ph.D., Thesis Committee Chair

Laszlo Kovacs Ph.D., Committee Member

Paul Durham Ph.D., Committee Member

Julie Masterson, Ph.D., Dean of the Graduate College

In the interest of academic freedom and the principle of free speech, approval of this thesis indicates the format is acceptable and meets the academic criteria for the discipline as determined by the faculty that constitute the thesis committee. The content and views expressed in this thesis are those of the student-scholar and are not endorsed by Missouri State University, its Graduate College, or its employees.

ACKNOWLEDGEMENTS

TABLE OF CONTENTS

LIST OF TABLES

LIST OF FIGURES

INTRODUCTION

Membrane fusion plays an essential role in critical intracellular processes such as organelle biogenesis, neurotransmission, and hormone secretion, as well as supporting the various stages of endocytic and exocytic traffic (Wickner & Schekman, 2008). Fusion is initiated as two opposing membranes are situated in close proximity to one another, followed by the local distortion of each individual lipid bilayer and their subsequent merger into a single membrane (Chernomordik & Kozlov, 2008). Various types of membrane fusion events coordinate cellular activities and are necessary for proper cellular functions. Homotypic vacuolar fusion is critical for regulating the degradation and recycling of materials needed to control cellular metabolism (Malia & Ungermann, 2016), while heterotypic endosome-to-Golgi fusion is necessary for recycling sorting receptors (Progida & Bakke, 2016). The well-characterized SNARE-mediated {(soluble N-ethylmaleimide–sensitive factor) - attachment protein receptor)} vesicle fusion with the plasma membrane acts as a central regulator for neurotransmitter release (Südhof & Rizo, 2011).

While specific molecular components differ between the many unique multimeric protein interactions required for each localized fusion event, target and vesicular SNARE interactions (*t*-SNAREs and *v*-SNAREs, respectively) generally comprise the central machinery necessary for fulfilling the proximal requirements to initiate fusion (Han *et al*, 2017). Associated SNARE complexes force two individual membranes into proximal arrangements that cause the apposed bilayers to come into direct contact with one another. It was long speculated that SNARE proteins alone could drive the entire process of fusion (Weber *et al*, 1998). While SNARE interactions are critical for the proximal requirements between two fusing membranes, SNARE

1

assembly alone is insufficient to mediate the entire synaptic fusion cycle (Südhof, 2013a). Thanks to breakthroughs in *in vitro* lipid and content mixing analysis using artificial proteoliposome constructs, the current paradigm surrounding fusion mechanics now incorporates a host of local protein interactions required for full fusion. The specific proteins involved include Rab's and their effector proteins, tethers and adaptors, chaperones, as well as specialized lipids with fusogenic properties (Wickner & Rizo, 2017). Studies using isolated yeast vacuoles and reconstituted proteoliposomes carrying florescent lipids in the presence of these protein components have supported this new paradigm in various *in vitro* fusion reconstitution assays. In these assays, it was shown that vacuolar lipid and content mixing, through SNARE activity alone, was only observed at high SNARE densities far outside normal physiological concentrations, and fusion at physiological SNARE densities required Rab GTPase Ypt7 imbedded in both fusing membranes (Zick *et al*, 2015).

Taken together these finding provide strong support for the necessity of a localized protein network, including SNARES and additional factors, acting synergistically to regulate the assembly/disassembly cycles during SNARE complex formation and SNARE-mediated fusion. A unified mechanism uniting the numerous spatiotemporal protein and lipid interactions required for fusion has yet to be proposed and seems unlikely due to the diverse protein networks and interactions specific to each precise fusion event. The following is meant to elucidate the diversity and complexity inherent in various types of membrane fusions by highlighting similarities and differences, as well as the recent advances specific to each type of fusion reaction being discussed. The yeast and mammalian SNARE and SM proteins for each type of fusion reaction are listing in Table 1.

Synaptic Membrane Fusion

The precision and speed required for neurotransmission is tightly controlled by fusion events that regulate neurotransmitter release via neuronal exocytosis. During synchronous release, voltage-gated Ca^{2+} channels briefly open triggering a localized influx of Ca^{2+} that binds to the calcium sensor synaptotagmin-1 at presynaptic active zones inducing Ca^{2+}-triggered fusion pore opening and content release of neurotransmitter-filled synaptic vesicles to the presynaptic plasma membrane. (Südhof & Rizo, 2011). Before pore opening and expansion, which represent later stages of the complete fusion cycle, loaded vesicles must be docked close to cargo release sites. The specific proteins and molecular mechanisms of this docking step need further elucidation, but interestingly SNAREs do not appear to be involved in this process. After docking, synaptic vesicles are primed for fusion via the activation of syntaxin-1 from its closed conformation to the open Munc18-binding confirmation that promotes the partial assembly of the trans-SNARE complex (Dawidowski & Cafiso, 2016).

Interactions between the coiled-coil regions of presynaptic membrane SNAREs, syntaxin-1, SNAP-25, and *v*-SNARE synaptobrevin form a partially "zippered" conformation representing the initial fusion intermediate step (Gundersen, 2017). Partial trans-SNARE complex formation is followed by progressive zippering from the N- to C-terminal of the four-helical bundle (Südhof & Rothman, 2009). SNARE complex assembly is enhanced by molecular chaperones (CSPs and synucleins), while disassembly is maintained by N-ethylmaleimide-sensitive factor (NSF) and SNAP protein adaptors (α-, β-, or γ-SNAP) (Rizo & Xu, 2015; Söllner *et al*, 1993). In 2013, the collaborative Nobel Prize winning work of James Rothman, Randy Schekman, and Thomas Südhof revealed that proper synaptic fusion requires SNARE-associated SM proteins (Sec1/Munc18-like proteins) aided by chaperone complexes, NSF-

cysteine string proteins (CSPs) and synucleins, localized to active zones at the site of synapsis (2013). Results from further studies have supported the necessity of accessory proteins and demonstrated that SNARE activity alone can drive the hemifusion step, but synaptotagmin (Syt1) and Ca^{2+} were required for full fusion and pore expansion during rapid neurotransmitter release (Lai *et al*, 2013; Liu *et al*, 2016).

During hemifusion, only the outer leaflets of each bilayer participate in lipid mixing, while the inner leaflets remain distinctly separate. Full fusion is marked by the continuation of lipid mixing through both leaflets and the opening and expansion of a fusion pore, which facilitate content release and the physical coalescence of the two previously distinct bilayers (Giraudo *et al*, 2005). As previously mentioned, assembly chaperones (CSPs and synucleins) enhance SNARE complex assembly, while the progressive zippering of the trans-SNARE complex forces the two-apposed bilayers into close proximity resulting in the destabilization of both membranes around the active fusion site. As the fusion pore expands the *trans*-SNARE complex, marked by fusion machinery separately associated with each membrane, converts to a *cis* conformation in which the associated SNARE-SM proteins reside on the same merged membrane (Südhof, 2014; Martens & McMahon, 2008).

A new paradigm proposed by Jose Rizo and William Wickner also focuses on the necessity of effector proteins bound to the *trans*-SNARE complex during the later stages of fusion. These various effectors trigger lipid rearrangement by inserting their apolar domains into the bilayer completing the last discernable steps of fusion (Wickner & Rizo, 2017). After fusion, disassembly of the SNARE complex is regulated by the ATPase NSF protein, which binds SNARE complexes via SNAP protein adaptors. ATP hydrolysis provides the energy for

disassembly of the subsequent *cis*-SNARE complex and frees the SNAREs for later rounds of *trans*-SNARE associations (Söllner *et al*, 1993; Wickner & Rizo 2017).

Homotypic Vacuolar Fusion

Vacuolar fusion retains many functional similarities when compared to the previously mentioned model of synaptic membrane fusion. The most obvious dissimilarity between the two fusion events is the use of calcium-gated channels mediated by the Ca^{2+} sensor synaptotagmin to achieve the precise millisecond precision necessary for rapid neurotransmitter release (Fernandez-Chacon *et al*, 2001; Südhof, 2013b). In yeast, vacuolar fusion microdomains, which were found to be enriched with fusogenic proteins and lipids that facilitate membrane fusion, include SNAREs, Rab GTPases (Barr, 2013) and their exchange factors, effectors, tethering complexes, associated SM proteins (Lürick *et al*, 2016; Baker *et al*, 2015), and a variety of fusogenic lipids (Fratti *et al*, 2004; Mima *et al*, 2008; Orr *et al*, 2015; Zick *et al*, 2015).

Many *in vitro* reconstitution assays using purified vacuolar membranes and synthetic proteoliposomes have provided powerful evidence for a multitude of localized proteins, in addition to SNAREs, necessary for efficient fusion under near physiological conditions (Wickner & Rizo, 2017; Zick & Wickner, 2016; Baker & Hughson, 2016). During vacuolar homotypic fusion, the hexameric homotypic fusion and vacuole protein sorting (HOPS) complex acts as a tether directly binding to Rab/Ypt7 located on apposed membranes. Membrane bound Rab/Ypt7, a GTPase switch-like protein, is necessary for the proper localization of HOPS to the site of fusion and requires guanine nucleotide exchange factors (GEF$_S$) for their activation to the GTP-bound functional form (Barr, 2013). The HOPS core complex is composed of four subunits (Vps11, 16, 18, and 33) and two specific Rab binding subunits (Vps41 and Vps39). The latter

two are located at opposite ends of the complex and are thought to fulfill bridging requirements by closely positioning each of the apposed membranes' SNAREs for *trans*-SNARE complex formation (Kummel & Ungermann 2014; Brocker *et al*, 2012).

SNAREs can be categorized as R- (arginine) or Q- (glutamine) based on the central arginyl or glutaminyl residues located in the heptad-repeat SNARE domains (Fasshauer *et al*, 1998; Kloepper *et al*, 2007). The four SNAREs that participate in vacuolar fusion are R-SNARE Nyv1, Qa-SNARE Vam3, Qb-SNARE Vti1, and Qc-SNARE Vam7. The Qc-SNARE Vam7 is the only peripheral SNARE that binds to membranes based on affinities for acidic lipids, as well as HOPS and other SNAREs. The other three SNAREs (R-, Qa, Qb) are membrane anchored by a C-terminal transmembrane domain (TMD) (Lee *et al*, 2006; Stroupe *et al*, 2006; Karunakaran & Wickner, 2013). The HOPS subunit Vps33 is an SM-like protein with a characteristically conserved groove that binds R- and Qa-SNAREs (Baker *et al*, 2015). X-ray structures have shown Qa-SNARE Vam3 lies in the conserved cleft of Vps33, while R-SNARE Nyv1 binds to a non-overlapping region outside the cleft. The initial interaction between Vps33 and Vam3 is thought to bind and facilitate the unfolding of Vam3 at the N-terminus, from a closed to an open Qa-SNARE motif capable of binding Nyv1 and allowing further SNARE complex assembly. Vps33 is then thought to act as a molecular chaperone by managing the interaction between R-SNAREs, located on the apposed bilayer, and the open (primed) conformation of Qa-SNAREs though the precise mechanisms of these interactions are somewhat unclear (Baker *et al*, 2015; Baker & Hughson, 2016). Importantly, both R- and Qa-SNARE motifs can simultaneously bind Vps33 and orient themselves in the same direction (N-to-C). Both SNAREs also align with each other in the same register when bound to Vps33, with their central zero-layer residues proximal to one another. Lastly, removal of the Vps33 region that interacts with the N-terminals of both

Nyv1 and Vam3 disrupted binding between the SM protein and SNAREs, though this mutant could still stably fold, bind Vps16, and incorporate into the HOPS complex (Baker *et al*, 2015; Zick & Wickner, 2016). These data strongly support the function of Vps33 acting as an SM-like protein by chaperoning the interactions between R- and Qa-SNAREs during *trans*-SNARE complex assembly.

Endosome Derived Golgi Fusion

While synaptic and vacuolar fusion have been well characterized, the mechanisms of endosome-to-Golgi fusion are far less understood. In yeast, Vps45 and Sly1, are the two known SM-like proteins primarily functioning at the Golgi. Both Vps45 and Sly1 share similar regulatory functions when compared to Munc18-1 and Vps33, mainly in chaperoning the open/closed conformations of syntaxin-like Qa-SNAREs Habc domains. Unlike the previously described SM-SNARE interactions, Vps45 and Sly1 do not participate in further steps of *trans*-SNARE complex pairing or alignment. In fact, both Vps45 and Sly1 share similar binding mechanisms interacting with the N-terminal regions (N-peptide) of Golgi Qa-SNAREs Tlg2 and Sed5, respectively, proceeding the Habc domain (Burkhardt *et al*, 2008; Furgason *et al*, 2009; Demircioglu *et al*, 2014). Furthermore, nuclear magnetic resonance (NMR) studies did not reveal a closed conformation adopted by Tlg2p, although a key N-terminal portion of the SNARE motif was missing from the bacterial purified construct used in this analysis. This arguably could affect the SNARE motif interactions present in the closed auto-inhibitory conformations seen in other Qa-SNAREs of the syntaxin family (Dulubova *et al*, 2002; Furgason *et al*, 2009; MacDonald *et al*, 2010).

High resolution structural analysis will be necessary to further assess the exact mechanisms by which Vps45 chaperones the closed conformation of Tlg2. Additionally, while many *in vivo* and *in vitro* assays support the SM-like function of Vps45 in fusion, there are currently no lipid or content mixing assays to test this assertion.

Understanding the Limitations of Fusion Assays

Interpreting the various and sometimes conflicting results of different fusion assays relies on understanding the strengths and limitations of the specific assays employed as well as the quality and specificity of data that can be gleaned from them (Chen *et al*, 2006). Reconstituted membrane fusion depends on the physical state of the membranes, proper SNARE incorporation and pairing, and accessory protein factors such as tethers, Rab's, and SM's to achieve efficient fusion at near physiological concentrations of proteins (Zucchi & Zick 2011; Wickner & Rizo, 2017). As previously mentioned, early liposome fusion assays conducted with SNARE's alone required excessive amounts of SNARE proteins loaded on the membrane surface to achieve significant rates of fusion (Weber *et al*, 1998; Paumet *et al*, 2001). These early fusion assays were primarily quantified using lipid mixing strategies and did not incorporate a measure of full fusion as in the protected luminal content mixing assays. Lipid mixing assays are generally measured using fluorescently tagged lipids and mixing is monitored by observing the increase in fluorescence of a quenched lipid (NBD-PE), as membrane mixing will dilute the fluorophores and allow dequenching from the quenching lipid (Liss Rhod-PE) (Weber *et al*, 1998). One major limitation to interpreting the lipid mixing assay is that fluorescent dequenching can arise from membrane lysis and reannealing, hemifusion where only outer leaflets mix, as well as full fusion and protected content mixing. Content mixing assays were first developed using small molecules

such as 1-aminonaphthalene-3,6,8-trisulfonate (ANTS), a polyanionic fluorophore, and alpha'-dipyridinium p-xylene dibromide (DPX), a cationic quencher, loaded into separate *t* and *v*-SNARE liposome populations (Smolarsky *et al*, 1977). Content mixing is then monitored by measuring the quenching of ANTS fluorescence by DPX upon fusion pore opening and the luminal mixing of the two previously separated molecules. Methods for content mixing now commonly utilize fluorescently conjugated protein with high affinities, such as streptavidin and biotin, and content mixing is measured via the increased buildup of FRET between the fluorescent tags (Cy5 and PhycoE, respectively). More recently, reconstituted fusion assays have been developed that can measure both lipid and content mixing simultaneously (Zucchi & Zick 2011; Liu *et al*, 2017). The obvious advantage of this assay is the ability to relate lipid mixing data to full fusion and content mixing information simultaneously using the same liposome populations. The simultaneous assay also has the added benefit of being able to quantify what percent of monitored fusion may occur from lysis or leakiness of the membranes and not true fusion mechanisms. In these assays, free/external unlabeled streptavidin is added in excess to control wells so that any biotin-PhycoE released from the liposomes due to lysis or leakiness immediately binds to unlabeled streptavidin preventing a FRET signal. The numerous advantages of the simultaneous assay have made it a strong model for analyzing the multiple stages of the fusion reaction and interpreting those results with a higher level of confidence than the data gained from lipid mixing alone. While the simultaneous assay is gaining considerable traction in its implementation; lipid mixing assays are still considered the standard and are frequently used primarily because they are cheaper, far easier to implement, and data collection and analysis is more straight forward.

The method of liposome formation, as well as SNARE density, can also negatively or positively effect fusion. Among the many liposome formation procedures, the standard method involving comicellization of lipids and proteins and the direct method of incorporating detergent-solubilized proteins into the preformed liposomes are widely used for SNARE reconstitutions into proteoliposomes. While the direct method produces more homogenously sized liposome populations, their propensity to fuse is considerably less than liposomes prepared by the standard comicellization method (Chen *et al*, 2006).

The higher propensity for liposomes to fuse when generated by the standard method may be due to the inconsistent size distributions of these liposome populations. Liposomes produced by the direct method are of very uniform sizes (~100nm), whereas liposome populations produced by comicellization exhibited more variable sizes (~50-125nm). Furthermore, liposomes with high SNARE densities produce vesicles considerably smaller in size than the average secretory vesicles and are prone to create particles of very small sizes (<10nm) that are more likely to be micelles than vesicles. It is hypothesized that the small size of these liposomes produces high geometric curvature resulting in substantial curvature stress on the membrane. Theoretically, this negative curvature stress will cause the liposomes to be more prone to stalk formation and fusion as to relieve the stress on the membrane (Chen *et al*, 2006). This, in addition to the excessive SNARE densities that may be present on such small vesicles or micelles, may be the reason for the increased lipid mixing found in fusion assays produced by the standard method of comicellization.

The method of dialysis is also believed to be of considerable importance in preserving the integrity of the membrane of reconstituted proteoliposomes. Some early fusion assays used large 4L buffer tanks to dialyze many samples simultaneously overnight without buffer or adsorbent

bead exchanges (Weber *et al*, 1998; Paumet *et al*, 2004). Newer simultaneous methods have stressed the importance of changing buffers, temperatures, and buffer volumes during the dialysis procedure for proper liposome formation and increased membrane integrity (Liu *et al*, 2017).

The Dynamin-Related Protein, Vps1, and Membrane Fusion

While Vps1 has traditionally been characterized as a membrane fission protein, its role in fusion has only been minimally explored (Peters *et al*, 2004; Alpadi *et al*, 2013; Kulkarni *et al*, 2014). Recent structural studies of Vps1 have shown that it primarily localizes and functions at endosomal compartments and self assembles into long helical structure in the presence slowly hydrolysable GTP analogue, guanylyl-(alpha, beta)-methylene-diphosphonate (GMPCPP) (Varlakhanova *et al*, 2018). Studies from our lab have found that Vps1 interacts with Vps51, a subunit of the GARP tethering complex, through two residues that are conserved in the human Vps51 homolog (Ang2) and mutation of these residues resulted in retrograde trafficking defects of endosomal SNARE Snc2 (Saimani *et al*, 2017). Further studies from our lab have shown that Vps1 interacts with Snc2 and Vti1 in Yeast-2-Hybrid (Makaraci *et al*, 2018) though theses interaction could not be validated using GST-pulldowns with the purified SNARE proteins and Vps1p (unpublished data). Vps1 has also been proposed to play a role in vacuolar membrane fusion by sequestering an available pool of Qa-SNARE Vam3 and facilitating it's interaction with the HOPS complex (Alpadi *et al*, 2013). Further research from the same lab later suggested a mechanism by which Vps1 facilitates the transition from hemifusion to content mixing through the oligomerization of Vps1 and its binding to the SNARE domain of Vam3 to increase the number of available Qa-SNAREs for fusion. While these assays assert a role for Vps1 in

vacuolar membrane fusion, no other research has validated these findings and Vps1's involvement in endosomal fusion has not been investigated using reconstituted fusion assays.

For these reasons, my thesis project involved the development of both lipid mixing and simultaneous lipid and content mixing assays using reconstituted proteoliposomes to measure the competency of SNARE-mediated endosome-to-Golgi retrograde fusion in yeast. The assays include proteoliposomes harboring yeast endo-to-TGN SNARE proteins (Snc2p, Tlg2, Tlg1, Vti1) and the dynamin-related protein Vps1. These *in vitro* reconstitution assays will be used to characterize the mechanism by which Tlg2 is activated for full fusion and content mixing as well as the role of Vps1 in the fusion reaction. My findings presented here could eventually help elucidate the specific mechanisms by which SM's and other accessory proteins regulate SNARE-dependent endosome-to-Golgi fusion.

MATERIALS AND METHODS

For my study, yeast endosome-to-*trans* Golgi Network (TGN) SNARE proteins were reconstituted into fluorescently labeled liposomes to assess their fusion efficiency in the presence of Vps1 and nucleotide. Briefly, purified yeast SNARE proteins were isolated from *E. coli* using recombinant protein technology and inserted into liposomes by detergent-based methods. Lipid mixing was quantified by measuring the fluorescent dequenching of NBD labeled lipids from rhodamine-labeled as described in Weber *et al*, 1998 and Paumet *et al*, 2001. Later simultaneous fusion assays incorporated a measure of content mixing and/or leakiness that was monitored by the increased FRET signal of Cy5-streptavidin and PhycoE-biotin as in Zucchi and Zick, 2011 and Liu *et al*, 2017.

All genes for the yeast recombinant proteins being studied (Vps1p, Tlg1p, and Snc2p) were first inserted into plasmids containing Histidine (His) or Glutathione-S-Transferase (GST) tags and the recombinant vectors were transformed into *E. coli*. Competent *E. coli* cells were used to express the recombinant proteins of interest, and affinity chromatography was used to purify and isolate individual SNAREs and accessory proteins. The purified SNAREs were reconstituted into proteoliposomes containing fluorescently labeled lipids, nitrobenzoxadiazole (NBD) and lissamine *rhodamine* B (Liss Rhod), using a detergent-based reconstitution strategy.

After reconstitution, fusion efficiency was assessed by measuring the dequenching of NBD fluorescence in the presence of the additional protein being studied (Vps1) and nucleotide over two hours. Simultaneous assays were conducted by measuring dequenching of NBD florescence and the buildup of FRET between Cy5-streptavidin and PhycoE-biotin in the presence of Vps1 and nucleotide for three hours.

Small Scale Protein Expression

All plasmid constructs were first tested under small-scale conditions to optimize the best parameters for protein expression in subsequent large-scale purifications. The method to test all constructs followed these same general parameters, except for kanamycin and chloramphenicol, which were used as selective antibiotics for plasmids introduced into Rosetta (DE3) pLysS (his$_6$-3C-Tlg1p, his$_6$-3C-Vti1p, and his$_6$-3C-Snc2p). After introduction of pET6xHN vector harboring the DNA sequence for Vps1 into SoluB121 (DE3) competent *E. coli* strains, positive colonies were confirmed by restriction digest and inoculated into 3 mL starter cultures of terrific broth (TB) with a working concentration of 100 μg/mL carbenicillin at 37 °C overnight with shaking (250 rpm). The overnight samples were diluted in a 1:20 ratio with a fresh 5 mL culture of terrific broth and carbenicillin the following morning and allowed to grow to an OD of ~0.6 measured at 600nm. The 5 mL cultures were then split into 2 mL uninduced (UI) samples and 3mL induced (I) samples. The induced samples were inoculated with 1 mM Isopropyl β-D-1-thiogalactopyranoside (IPTG) and both UI and I samples were incubated on ice for 15 minutes with vigorous shaking every few minutes. After the ice incubation, both UI and I samples were tested for protein expression at standardized temperatures of 24 °C, 30 °C, 37 °C, and sometimes 16 °C when necessary (for 10hr, 7hr, 4hr, and 20hr respectively) shaking at 280 rpms. The UI and I samples were then pelleted by centrifugation in a table top centrifuge (Beckman J2-HS) for 20 minutes at 4 °C and 3000xg. The supernatant was removed by decanting, and the pellet was resuspended and lysed by pipetting with 500 μL 1xPBS (Phosphate Buffered Saline, pH 7.4) and 100 μL 2x or 5xSDS (Sodium Dodecyl Sulfate) lysis buffer. The sample was then sonicated using a Branson 250 sonifier fitted with a titanium ultra-high tapered microtip for ~45sec-1min with output controls set to 2-3 and one second bursts. The sonicated samples were heated to

95 ℃ for 5 minutes using a hot plate and clarified by centrifugation at max speed (13,000xg) for 15 minutes two times. After centrifugation, 15 μL of the supernatant was carefully harvested from the very top of the centrifuge tubes and applied to an SDS-PAGE gel for visualization. The SDS-PAGE gel was loaded with UI and I samples side by side of the same protein variants and temperatures to compare the best expression conditions for large-scale purifications. All SDS-PAGE gels were stained with Coomassie blue for 7 minutes and destained for one-hour rocking at room temperature. Then, the destain buffer was changed and the gel was left rocking overnight for analysis the next morning.

His-tagged Protein Expression and Purification

The his_6-3C-Tlg1p, his_6-3C-Vti1p, and his_6-3C-Snc2p constructs were kind gifts from Dr. Joji Mima (Osaka University). These three constructs were introduced into Rosetta (DE3)pLysS *E. coli* chemically competent cells (Novagen) containing the additional pLysS plasmid for expression of rare eukaryotic codons. All the transformed strains and conditions for protein expressions were first developed in small-scale trials before subsequent large-scale purification procedures. The transformed cells were inoculated into 3 mL starter cultures of terrific broth containing 34 mg/mL chloramphenicol and 50 mg/mL kanamycin for the three SNARE constructs. The starter cultures were left to grow overnight at 37 ℃ in a shaking incubator at 220 rpm. The 3 mL starter cultures were then used to inoculate 500 mL sample cultures of TB containing the same working concentrations of antibiotics as previously mentioned. The sample cultures were allowed to grow in a shaking incubator at 37 ℃ (280 rpm) to an optical density of 0.6 (at 600 nm). Once the samples reached an OD of 0.6, the 500 mL culture was induced with IPTG at a 1 mM working concentration. For his_6-3C-Tlg1p and his_6-3C-Vti1p, the induced

samples were grown at 37 ℃ for 3.5 hours, while his$_6$-3C-Snc2p was induced at 16 ℃ for 20 hours, and 6xHN-Vps1 at 30 ℃ for 6 hours. The induced cultures were collected and evenly decanted into two pre-weighed 275 mL Sorvall centrifuge bottles. The Sorvall bottles were then centrifuged at 4000xg in a Beckman J2-HS centrifuge outfitted with a JA-14 rotor for 20 minutes at 4 ℃. After spinning, the supernatant was decanted off and the bottle was reweighed to calculate the left-over pellet weight (generally ~1.5 g). The pellets were then snap frozen by submerging the bottles in liquid nitrogen and immediately stored at -80 ℃ until the time of purification.

To purify the recombinant proteins from *E. coli,* the pelleted cells were chemically lysed by pipette using 2 mL of xTractor buffer (Clontech) per 100 mg of cell pellet, 5 μL DNase I (50U/μl, Thermo Scientific) per 1 g cell pellet, and 200 μL per 1-gram cell pellet of Lysozyme (10 mg/mL, Acros). The lysis mixture was pipetted until the pellet was thoroughly disrupted and protease inhibitors were added at the following working concentrations; 0.2 mM PMSF, 3.2 μM Bestatin, 1 μM Pepstatin A, 2 μM Leupeptin, 1.54 μM Aprotinin. Due to its short half-life, additional PMSF was added after clarification of the sample by centrifugation, during incubation with His60 Ni resin (Clontech), and to the dialysis buffer during overnight dialysis. The lysed sample was then transfer to a clean 50 mL polycarbonate centrifuge tube (Beckman Coulter) and completely submerged in a 200 mL glass beaker packed with ice for sonication. The 50 mL tube was sonicated on ice using a Branson 250 sonifier fitted with a titanium ultra-high tapered microtip for 1 minute 30 seconds with output controls set to 3 amps and intermittent 1 second bursts. The sonicated samples were then centrifuged in the same 50 mL tubes using a Beckman JA-20 rotor at 15,000xg for approximately 30 minutes or until the supernatant was completely clarified and free of cellular debris. The clarified supernatant was then decanted through a cheese

cloth (making sure not to disrupt the pelleted cellular material) into 50 mL falcon tubes for incubation with His60 Ni resin. The clarified supernatant containing the expressed recombinant proteins was incubated by rocking at 4 °C for 2 hours with 1-2 mL of His60 Ni resin in 50 mL Falcon tubes.

After incubation the protein lysate and resin mixtures were transferred to 10 mL disposable gravity columns (Bio-Rad) and the lysate was passed through the column to pack the resin. The resin was first equilibrated using 10 mL of equilibration buffer (Clontech) per 1 mL of resin making sure to never allow the column to run dry. After equilibration, 10 mL of binding buffer (Clontech; made by mixing 7.1 parts equilibration buffer with 0.9 parts elution buffer) per 1 mL of resin was added to the column and allowed to pass through the column, followed by 10 mL of elution buffer (Clontech) per 1 mL of resin. All flow through samples were collected and saved for validation using SDS-PAGE and visualized with Coomassie blue staining. Eluted samples were pooled based on concentration and purity prior to dialysis against 50 mM Tris-buffer containing 10% glycerol. Dialyzed protein samples were concentrated based on the desired concentrations using 6 mL Pierce concentrators (Thermo Scientific) that were at least half the molecular size of the purified protein (10 kDa, 30 kDa, and 70 kDa). Protein concentrations were quantified using a Qubit protein assay kit (Invitrogen) and samples were snap frozen in liquid nitrogen and stored at -80 °C in 20% glycerol for long-term storage.

GST-tagged Protein Expression and Purification

The GST-Tlg2 plasmid was constructed and introduced into SoluBL21 *E. coli* competent strains by fellow graduate student Ehsan Suez. After small scale trails to test for expression conditions, the transformed cells were inoculated into a 3 mL starter culture of TB media

containing 100 μg/mL of carbenicillin and allowed to grow overnight in a shaking incubator at

37 ℃ (230 rpm). The starter culture was used to inoculate a fresh 500 mL culture of TB media

contain 100 mg/mL of carbenicillin and incubated at 37 ℃ shaking at 280 rpm until the culture

reached an OD of 0.6 (600nm). While on ice, 1mM of IPTG was added to the 500 mL culture

and it was vigorously shaken every few minutes for a 15-minute ice incubation. The 500 mL

culture was then placed in a shaking incubator (280 rpm) and grown at 30 ℃ for 6 hours to

express the GST-Tlg2 recombinant protein. After induction, the sample was transferred into two

pre-weighed 275 mL Sorvall centrifuge bottles and centrifuged at 4000xg in a JA-14 rotor for 20

minutes at 4 ℃. The pelleted samples were reweighed, snap frozen, and stored at -80 ℃ as

described in the previous section.

The pelleted samples were lysed by pipetting and vortexing on ice with 50 μL of 1xPBS

per 1 mL of starting sample culture containing 1 mM Dithiothreitol (DTT). Once the pellet was

thoroughly resuspended, 150U per 1 gram of pellet of DNase1 (50U/μL) was added along with

200 μL per 1 gram of pellet of Lysozyme (10 mg/mL) and the sample was incubated on ice for 1

or 2 minutes with intermittent vortexing. Protease inhibitors (PMSF, Bestatin, Pepstatin A,

Leupeptin, Aprotinin) were added to the lysed samples in the exact same concentration and at the

same times as mentioned in the previous section. The lysed sample was transferred to 50 mL

polycarbonate centrifuge tubes and submerged in a 200 mL beaker filled with ice for sonication.

Sonication was performed using a Branson sonifier 250 exactly as previously described. The

sonicated sample was clarified by centrifugation at 15,000xg and 4 ℃ for approximately 30

minutes in a Beckman JA-20 rotor or until the sample was completely free of cellular debris. The

clarified sample was then decanted through cheese cloth, taking care not to disturb the pellet, and

filtered with a 0.45 μm sterile filter (FisherBrand) into a 50 mL Falcon tube.

The recombinant GST-Tlg2 protein was purified using a GSTrap HP column (GE healthcare) prepacked with 5 mL of Glutathione Sepharose High Performance resin. For low pressure liquid chromatography, a peristaltic pump with adjustable rotation speeds was used with size 14 rotor head and tubing (Masterflex). All flow rates were precalibrated on the pump using 1xPBS buffer and the GSTrap column before protein was loaded into the column. The column was first equilibrated with 8 bed volumes of binding buffer (10mM PBS pH 7.4) using a 10 mL/min flow rate making sure to never allow the column to go dry. The clarified lysate was then passed through the column for incubation with the resin by lowering the flow rate to 0.2 mL/min. After incubation, the column was washed with another 8 column volumes of binding buffer (10mM PBS pH 7.4) using a 5 min/mL flow rate. The column was eluted with 8-15 mL of 50 mM Tris buffer (pH 8) containing 15 mM of freshly added glutathione and lowering the flow rate to 1-2 mL/min. The eluted sample was captured in 1 mL fractions and analyzed using SDS-PAGE and Coomassie blue staining as previously mentioned. The 1 mL fractions were pooled based on protein concentration and purity and were dialyzed and saved in the same fashion as described early.

Lipid Mixing Proteoliposome Reconstitutions

All lipids for proteoliposome reconstitutions were purchased from Avanti Polar Alabaster, Alabama. The proteins used for reconstitutions were expressed and purified as previously described. Glass Gastight syringes (Hamilton) with PTFE Luer Locks were used for handling all lipids solubilized in chloroform as it will degrade plastics and leave impurities in the lipid solutions. The syringes were cleaned with 10 passes of acetone followed by 10 passes of chloroform before and after each use. Donor fluorescent liposomes bearing the *v*-SNARE his$_6$-

3C-Snc2p were prepared by premixing 6 mM lipid stocks in chloroform to make a 200 μL

solution in clean 16 x 125 mm glass test tubes prerinsed with chloroform. All the lipids used for

the fusion assay were 18:1 dioleoyl variants: DOPC (1,2-dioleoyl-sn-glycero-3-phosphocholine),

DOPS (1,2-dioleoyl-sn-glycero-3-phospho-L-serine, sodium salt), NBD-PE (1,2-dioleoyl-sn-

glycero-3-phosphoethanolamine-N-7-nitro-2-1,3-benzoxadiazol-4-yl), and Liss Rhod-PE (1,2-

dioleoyl-sn-glycero-3-phosphoethanolamine -N-lissamine rhodamine B sulfonyl) prepared in a

82:15:1.5:1.5 molar ratio, respectively (Table 2). The mixed lipid solutions were then dried into a

lipid film under a gentle stream of nitrogen for 3-5 minutes and vacuum desiccated using a Bel-

Art plastic vacuum desiccator, 230 mm plate size (Cole-Parmer) for a minimum of one hour to

remove any remaining trace amount of chloroform.

For reconstitution of *v*-SNARE containing proteoliposomes, the dried lipid film was

dissolved in a 400 μL solution of reconstitution buffer (25 mM HEPES-KOH [7.4 pH], 400 mM

KCl, 1 mM DTT, 10% glycerol) containing 40 nM for initial trials or, 6 μM of his$_6$-3C-Snc2p for

later assay, and 1% octyl β-D-glucopyranoside (βOG), a nonionic detergent commonly used to

solubilize membrane proteins and lipids (Table 3). After addition of the protein/βOG-solution

the lipids were dissolved by gentle agitation flicking the test tube every couple of minutes at

room temperature until the lipid film was no longer visible and the solution appeared

homogenous. For vesicle formation, the homogeneous solution was then vortexed vigorously at

room temperature while 800 μL of reconstitution buffer was added drop-wise to the 400 μL

protein/lipid solution to rapidly dilute the βOG detergent below its critical micellar concentration

(CMC). The excess detergent was removed by extensive dialysis (Fisherbrand 6,000-8,000

nominal MWCO dialysis tubing) against 4 L of reconstitution buffer with 4 g of SM-2 Adsorbent

Bio-beads (Bio-Rad) for 2 hours at room temperature then incubated overnight at 4 ℃. All

separate reconstitutions were done simultaneously and dialyzed together with samples distributed evenly and the total volume of dialysate did not exceed 6 mL per 4 L of buffer.

The vesicles were recovered from the dialysis tubing by pipette and samples were remeasured to account for volume changes during dialysis. The ∼1.2 mL dialysate was gently and thoroughly mixed with an equivalent volume of 80% Nycodenz solution dissolved with reconstitution buffer in an 11 x 60 mm polypropylene ultracentrifuge tube (Beckman Coulter). The resulting 40% Nycodenz solution was then overlaid with 700 μl of 30% Nycodenz using a syringe by gently swirling the syringe tip above the 40% layer and very delicately overlaying the 30% Nycodenz over the top. A final 250 μL Nycodenz and glycerol free layer (i.e., reconstitution buffer) was applied over the 30% layer in the same fashion. Upon proper layering one should be able to see the three visibly separated layers before advancing to centrifugation. The ultracentrifuge tubes were then transferred to a TH-660 swing bucket rotor and centrifuged at 4 ℃ for 4 hours at 48,000 rpm in a Sorvall WX+ Ultracentrifuge (Thermo Scientific). After ultracentrifugation, vesicles were harvested from the 0/30% Nycodenz interface in 100-200 μL fractions and saved in 1.5 mL screw cap centrifuge tubes on ice in a 4 ℃ refrigerator. Samples were generally measured the next day but can be stored for ~3 days without significant loss of fusion efficiency.

The non-fluorescent acceptor liposomes bearing pre incubated t-SNARE bundles were prepared in essentially the same method as described above except the 200 μL lipid/chloroform solution was prepared with 15 mM DOPC and DOPS lipids premixed in an 85:15 molar ratio, respectively (Table 2). The mixed lipids were prepared in a glass test tube, dried under a gentle stream of nitrogen, and vacuum desiccated as previously mentioned for donor liposomes. To form t-SNARE bundles, the necessary SNAREs (his$_6$-3C-Tlg1p, his$_6$-3C-Vti1p, and GST-Tlg2)

were incubated for 16 hours at 4 ℃ in 1 mL of reconstitution buffer containing 40 nM concentrations for individual SNARE protein during initial trails and 2 μM concentrations for later fusion assays (Table 3). After SNARE incubation, 1% βOG (w/v) was added to the 1 mL reconstitution buffer containing the *t*-SNARE bundles and the assembled SNAREs were incubated for 25 minutes at 4 ℃. The solution containing βOG detergent was then used to gently dissolve the lipid film as before. For vesicle formation, the homogenized solution was vortexed vigorously at room temperature while 2 mL of reconstitution buffer was added dropwise to the 1 mL protein/lipid solution to rapidly dilute the βOG detergent below its critical micellar concentration. The vesicles were then dialyzed extensively against reconstitution buffer and SM-2 Bio-beads to remove any traces of βOG detergent as previously described. After dialysis, the vesicles were collected and measured volumetrically to account for changes during dialysis. The ~3 mL of dialysate was then evenly split into two ~1.5 mL fractions in 11 x 60 mm polypropylene ultracentrifuge tubes and each was thoroughly mixed with an equivalent volume (~1.5 mL) of 80% Nycodenz to create a 40% Nycodenz layer. The bottom 40% layer of the gradient was overlaid with 750 μL of 30% Nycodenz, then a final 0% layer of reconstitution buffer lacking glycerol and Nycodenz was added to the very top as previously described. The layers should be visibly separated before moving to floatation by ultracentrifugation. Acceptor proteoliposomes containing *t*-SNAREs were centrifuged with a TH-660 swing bucket rotor at 4 ℃ for 3 hours 40 minutes at 55,000 rpm in a Sorvall WX+ Ultracentrifuge and the vesicles were harvested from the 0/30% interface in 200 μL fractions.

To create control liposomes containing no SNARE proteins, the above methods were followed except no SNARE proteins were added to the reconstitution buffer solutions containing the 1% βOG detergent.

Lipid Mixing Fusion Assay

Lipid mixing assays were conducted in black Costar 96-well FlouroNunc plates (Thermo Scientific) unless otherwise mentioned in the figure descriptions. Into each well, 5 μL of *v*-SNARE containing donor vesicles was mixed with 45 μL of *t*-SNARE containing acceptor vesicles by gentle pipetting. The 96-well plates containing the mixed liposomes were then preincubated at 4 °C protected from light for 2 hours with gentle agitation. After incubation, 2.5 mM $MgCl_2$ was first added to both control and experimental samples, followed by 100 μM of all GTP variants (GDP, GTP, and GTγP) into the designated wells (Table 4). 6xHN-Vps1 was added last at a concentration of 1 μM, which was determined by using varying concentrations of Vps1 in previous pilot experiments. The samples were then incubated at 37 °C with gentle agitation for 8 minutes and placed in the fluorescent plate reader for 5 minutes at 37 °C to acclimate before readings were taken. Lipid mixing was measured by the dequenching of NBD-PE lipids from Liss Rhod-PE and NBD fluorescence was measured at 460 nm excitation and 538 nm emission with a 515 nm cutoff filter. Increasing NBD fluorescence was monitored by kinetic readings every 2 minutes for a total of 2 hours at 37 °C with shaking every 5 seconds before readings. After 2 hours, the plate was removed from the reader and 10 μL of 2.5% Triton X-100 and all samples were simultaneously mixed using a multichannel pipette. Endpoint readings were taken immediately and 10 minutes after Triton X-100 addition to solubilize the liposomes and determine the maximum lipid mixing signal. The resulting data were normalized, and fusion was quantified as the change in NBD signal within the initial and endpoint readings after Triton X-100 addition.

Simultaneous Lipid and Content Mixing Proteoliposome Reconstitutions

All lipids used for the simultaneous fusion assay were purchased from Avanti Polar Alabaster, Alabama. Before use, all lipid stock solutions were removed from the -20 ℃ freezer and allowed to equilibrate to room temperate in the dark. The proteins used for reconstitutions were expressed and purified as previously mentioned. Lipids were transferred from stock solution and mixed using a microdispenser with positive replacement glass capillaries (Drummond) in 16 x 125 mm glass test tubes that were prerinsed three times with chloroform. All tubes were wrapped in aluminum foil and kept out of light to avoid photobleaching and photo-oxidation of the lipids whenever possible. While both content mixing and lipid mixing vesicles were prepared simultaneously with equivalent lipid and protein concentrations, the two assays were reconstituted into separate vesicle populations and measured in parallel wells due to fluorescent interference of NBD with PhycoE/Cy5 FRET.

To create *v*-liposome populations for the lipid mixing assay 5 mM of total lipids (DOPC, DOPS, DOPE [1,2-dioleoyl-sn-glycero-3-phosphoethanolamine], Ergosterol, NBD-PE, and Liss Rhod-PE) were mixed in a clean glass tube at 39:19:19:20:1.5:1.5 molar % ratios, respectively (Table 5). To create *v*-liposomes populations for the content mixing assay the exact same concentrations were used except fluorescent lipids (NBD-PE and Liss Rhod-PE) were omitted and the extra three molar percent was added evenly to DOPC, DOPS, and DOPE as seen in Table 5. For both preparations, the mixed lipid solutions were dried under a gentle stream of nitrogen while swirling the test tube to create a lipid film at the bottom of the tube. The tubes were then wrapped in aluminum foil with a hole poked in the top and vacuum desiccated overnight to remove any trace chloroform. After overnight drying, both lipid films were hydrated with 420 μL of reconstitution buffer containing 2% βOG and vortexed vigorously for about 2

minutes to completely suspend the lipid film. The dissolved lipids were then incubated at room

temperature for 15 minutes then sonicated twice in a bath sonicator for 5 minutes each time. At

this step, the mixed lipids solutions can be snap frozen in liquid nitrogen and stored at -80 ℃ for

up to one month. Reconstitutions of v-SNARE proteoliposomes for lipid mixing were prepared

by adding 5 μM his$_6$-3C-Snc2p (29.45 μL) into 100 μL of reconstitution buffer containing 1 %

βOG and mixing the protein solution with 200 μL of the fluorescent premixed lipid solution and

an additional 170.55 μL of reconstitution buffer containing 1% βOG detergent (Table 6). The

mixed lipid/protein solution was then incubated at room temperature for 25 minutes with end

over end rotation. To prepare v-liposomes for content mixing, the reconstitution was carried out

using the same method except 200 μL of the premixed lipid solution lacking florescent PE lipids

was used and the 200 μL of reconstitution buffer containing 1% βOG was replaced with 200 μL

of a 16 μM Cy5-Steptavidin (THERMO) solution containing 1% βOG (Table 6).

To prepare t-liposome populations for both the lipid and content mixing assays, 5 mM of

total lipids (DOPC, DOPS, DOPE, Ergosterol) were premixed in a clean glass test tube in a

38:20:20:20 molar % ratio, respectively (Table 5). The lipids were dried into a lipid film and left

to vacuum desiccate overnight to remove any trace chloroform, exactly as before. After drying,

the lipid film was hydrated with 420 μL of reconstitution buffer containing 1% βOG while

vortexing vigorously for about 2 minutes until the lipids were completely suspended. Both

content and lipid mixing used the same 420 μL mixed lipid solution during the fusion assay. To

prepare t-SNARE bundles, 1 μM working concentrations of each SNARE protein (his$_6$-3C-

Tlg1p, his$_6$-3C-Vti1p, and GST-Tlg2) were mixed in a centrifuge tube and incubated for 16

hours with end over end rotation at 4 ℃ (Table 7). Before reconstitution, 1% βOG (w/v) was

added to the assembled t-SNAREs and they were again incubated at 4 ℃ for 25 minutes. Lipid

mixing liposomes were reconstituted by mixing the *t*-SNARE bundles with 200 μL of the 5 mM

premixed lipid solution containing 2% βOG and 120 μL of reconstitution buffer with 1% βOG

(Table 8). The protein/lipid solution containing βOG was wrapped in aluminum foil and

incubated at room temperature for 25 minutes using slow rotation. The reconstitution of *t*-

liposomes for the content mixing assay was prepared using a similar method except that the 120

μL of reconstitution buffer containing 1% βOG was exchanged for 120 μL of a 16.7 μM solution

of PhycoE-Biotin (Invitrogen) also containing 1% βOG (Table 8).

After incubations all samples were transferred to prewetted 6,000-8,000 MWCO dialysis

tubing for subsequent dialysis. The ∼500 μL liposome samples were then excessively dialyzed

for complete detergent removal against reconstitution buffer containing SM-2 beads. The

samples were first dialyzed at room temperature for one hour in 500 mL of reconstitution buffer

containing 1 g of SM-2 Bio-beads. After an hour, the 500 mL of dialysis buffer was exchanged

with fresh reconstitution buffer containing another 1 g of SM-2 beads and dialyzed at 4 ℃ for

two hours. A final overnight dialysis was prepared by transferring the dialysis bags to fresh

buffer tanks containing 1 L of reconstitution buffer and 2 g of SM-2 Bio-beads (Table 9). All

buffer tanks were wrapped in aluminum foil to prevent photobleaching of fluorescent lipids and

photo-oxidation. After dialysis, the ∼500 μL dialysate samples were collected by pipette and

transferred to 2 mL centrifuge tubes on ice for floatation gradient purification.

For proteoliposome purifications, the dialysate was volumetrically measured to account

for volume changes during dialysis and ∼450 μL of sample was collected for purification. The

∼450 μL samples were then mixed with reconstitution buffer to make a total of 900 μL.

Nycodenz stock solution were made for the floatation gradients in the following concentrations;

70% Nycodenz was dissolved in reconstitution buffer contain 2% glycerol, 25% Nycodenz was

prepared by diluting the previously made 70% Nycodenz in reconstitution buffer containing 10% glycerol. The 900 μL samples were thoroughly mixed by pipetting with an equivalent volume of 70% Nycodenz (making a 35% Nycodenz layer) and then transferred slowly into 11x60 mm polypropylene ultracentrifuge tubes. The 25% Nycodenz solution was then overlaid on top of the 35% layer using a syringe and slowly adding 1.6 mL of 25% Nycodenz carefully above the bottom layer. Lastly, 500 μL of a 0% Nycodenz layer containing 10 % glycerol was carefully overlaid above the 25% layer in the exact same fashion. After adding the Nycodenz gradients each individual layer was clearly visible prior to ultracentrifugation. The ultracentrifuge tubes were loaded into swing buckets for a TH-660 rotor and centrifuged at 55,000 rpm for 2 hours at 4 ℃ in a Sorvall WX+ ultracentrifuge. The liposome samples layers should be clearly visible after ultracentrifugation (Figure 1). The purified proteoliposomes were carefully harvested from the top interface in 500 μL fractions using a syringe and saved on ice in 1.5 mL screw cap centrifuge tubes wrapped in aluminum foil. The proteoliposome samples can be saved at 4 ℃ for 24 hours with no apparent loss of activity, or snap frozen and saved in liquid nitrogen or -80 ℃ with only ~10 % loss of activity (Liu *et al.*, 2017).

Simultaneous Fusion Assay

Lipid and content mixing assays were conducted simultaneously in parallel in black Costar 96-well FlouroNunc plates. For both assays, 5 μL of *v*-liposome was gently mixed by pipette with 45 μL of *t*-liposomes and allowed to incubate at 4 ℃ with gentle agitation covered in the dark for two hours. Blank control samples were prepared by mixing 5 μL of *v*-liposomes with 65 μL of reconstitution buffer to account for the final well volume of tested samples. After preincubation, 2.5 mM MgCl$_2$ was added to all loaded wells followed by 100 μM of the various

GTP variants (GDP, GTP, and GTγP) to their selective wells (Table 4). Reconstitution buffer was used to balance the volumes between wells, so all samples had the same final volume in each well. Vps1 was added last to all test wells in 1 μM final concentration and all samples were gently mixed in unison by pipetting with a multi-channel pipette. The 96-well plate was incubated at 37 °C with gently agitation covered from light for 8 minutes then placed in a SpectraMax M5 fluorescent plate reader for 5 minutes at 37 °C to acclimate before readings were taken. Kinetic readings were taken every two minutes at 37 °C for 3 hours with shaking for 5 seconds before each reading. Lipid mixing was monitored at 460 nm excitation and 538 nm emissions wavelengths as previously described in the lipid mixing fusion assay. Content mixing was quantified by the buildup of FRET between PhycoE-Biotin and Streptavidin-Cy5 during content release (excitation 565 nm, emissions 675 nm). To account for increased FRET due to vesicle leakiness and not true content mixing, replicate control wells for each of the content mixing conditions were loaded with 4 μM free unlabeled streptavidin to bind any PhycoE-Biotin released due to leakiness. After three hours, the plate was removed from the plate reader and 10 μL of 1% Triton X-100 was simultaneously mixed with each sample using a multi-channel pipette. Endpoint reading were taken after Triton X-100 addition to quantify total possible fluorescence for both content and lipid mixing assays.

Electroformation of GUV's on Pt-Wire

All lipids used for giant unilamellar vesicle (GUV) construction were purchased from Avanti Polar and GUV's were formed by electroformation on platinum wire in a custom-built chamber made in house (Figure 2a). The chamber was assembled by securing a silicone double-sided adhesive spacer (3M) to a 3" x 1" glass microscope slide and fixing the bottom well of the

chamber to the opposite side of the adhesive spacer (Figure 2b). The glass slides were preincubated in a solution of sterile water containing 3 mg/mL casein protein for 3 minutes and dried overnight before applying the adhesive. All glass slides making contact with liposomal membranes were incubated in casein to keep the GUVs from bursting when contacting shear glass. Silicone adhesive glue (3M) was then spread completely around the edge of the chamber to seal it from leaking during electroformation (Figure 2c).

Lipid stock solutions of 0.25-1 mg/mL were prepared for GUV formation by mixing DOPC, ergosterol, and NBD-PE in a 4 mL glass tube with PTFE liners in a 90:9:1 molar % concentration, respectively. All lipid solutions were prepared in a fume hood and handled with glass syringes as the lipids are solubilized and mixed in chloroform. When applying lipid deposits on to the platinum (Pt)-wires the lid of the electroformation chamber was placed in the mount (Figure 2d) to keep the electrodes stable. The lipid deposits were made with 2.5 μL of the lipid stock solution using a 5μL fixed needle Hamilton syringe with a beveled tip. For each electrode, 3-6 lipid droplets were deposited in as thin of layers as possible and dried under a very gentle stream of nitrogen, taking care not to disturb the droplet. The whole lid assembly containing the Pt-wire electrodes was placed in a vacuum desiccator and the lipids were dried of chloroform under vacuum pressure for two hours (Figure 2e).

The lipid droplets may be swelled in a variety of buffers, but for most electroformations GUVs were swollen in 10 mM Tris buffer (pH 7.4) containing 1 mM EDTA to accord with protein buffer conditions. The assembled bottom half of the chamber was checked for leaks and the function generator was warmed up by allowing it to run for 30 minutes at the desired amplitude before applying electricity to the Pt-wire electrodes. After inspection, the chamber was filled with 1.5 mL of the desired buffer and the lid of the chamber was secured to the assembled

bottom by screwing them together very slowly and carefully as to avoid disturbing the lipid deposits. Once the chamber was fully assembled, it was carefully placed in the chamber rack and the alligator clips were secured to the electrode posts making sure to be in direct contact with the Pt-wire (Figure 2f). The entire chamber and rack assembly was placed on ice for the formation procedure as the constant electric flow produces heat that can build pressure inside the chamber. For low ionic swelling buffers (10 mM Tris and 1 mM EDTA), step 1 of the electroformation was started with the amplitude at 0.5 Vpp (peak-to-peak) and hand ramped to 2 Vpp evenly over a 30-minute time period with a constant frequency of 300 Hz using a sine wave. After thirty minutes, the liposomes were allowed to swell (step 2) by electroformation at the same amplitude and frequency (2 Vpp and 300 Hz) for 90 minutes. For detachment of the GUV's from the Pt-wire, the frequency was abruptly dropped from 300 Hz to 50 Hz and then gradually dropped from 50 Hz to 2 Hz over a 30-minute period. The GUV's were allowed to detach under a constant amplitude of 2 Vpp and frequency of 2 Hz for an additional 30 minutes (Table 10) then the chamber was lightly tapped to detach any GUVs still clinging to the Pt-wire. GUVs were harvested using 1 mL large orifice pipette tips (Fisherbrand) to reduce shear force and bursting of the liposomes when being drawn though small diameter pipette tips due to their large size (1 μm-100 μm).

To visualize the success of GUV formations, glass slides coated with casein protein were prepared with double sided adhesive silicone spacers as previously mentioned but containing a hole punched through the center of the spacer. The well made from the hole punch was then filled to the top with the collected GUV solution (20-50 μL) and a cover slip secured to the opposite side of the adhesive silicon spacer was held in place for at least 1 minute to prevent leaking. The glass slide was then placed into an inverted spinning disk confocal microscope

(Olympus) and the GUVs were visualized using GFP wavelengths (Figure 3). Note: for these GUVs the premixed lipid solution contained NBD-PE (excitation/emission, ~463/536 nm), for vesicles formed with Liss Rhod-PE (excitation/emission, ~560/583 nm) instead of NBD-PE the GUVs should be visualized using RFP wavelengths.

RESULTS

Endosome-to-TGN SNAREs are Required to Stimulate Lipid Mixing *In Vitro*

Retrograde fusion of endosome-derived vesicles with the *trans*-Golgi membrane requires Tlg2, Tlg1, Vti1, and Snc2 to stimulate membrane fusion. The SNARE proteins were purified as recombinant proteins and visualized with SDS-PAGE gel electrophoresis and Coomassie blue staining (Figure 4). SNARE incorporation into liposomes was visually assesed using 10 μL of *v* or *t*-proteoliposomes in 200 μL Bradford assay buffer and by western blot using *v*-SNARE proteoliposomes containing Snc2p (Figure 5). Proteoliposome formations was visualized by confocal microscopy using RFP excitation for Liss-Rhodamine labeled proteoliposomes (Figure 6). While SNARE mediated fusion resulted in increased fluorescence compared to *v*-SNARE blank controls or empty liposomes, lipid mixing is modest and only accounts for ~10 % of the total fusion potential as judged after TritonX-100 addition. The addition of Snc2-C-terminal peptide showed only a modest increase of lipid mixing at low concentrations in preliminary assay (Figure 7) but this could not be replicated in later assays. In all later assays Snc2-C-peptide did not increase fusion when compared to SNARE only controls as reported in Paumet *et al*., (2001) and Paumet *et al*., (2004). Due to the ineffectiveness of the Snc2 C-terminal peptide in stimulating lipid and content mixing the data were omitted from subsequent fusion assays for clarity.

Vps1 Stimulates SNARE Mediated Endosome-to-TGN Lipid Mixing

The concentration of Vps1 used in both lipid mixing and simultaneous assays was determined by preliminary lipid mixing trails using increasing concentrations (10 nM, 100 nM,

and 1 μM) of Vps1 (Figure 8). Increasing concentrations of Vps1 was shown to stimulate lipid mixing in a concentration dependent manner with the 1 μM concentration facilitating the highest rate of lipid mixing (Figure 8). For all subsequent assays 1 μM concentrations were used as this protein concertation was similar to the SNARE concentrations used in later fusion assays (1 μM-3 μM). It is important to note that this concentration does not cause significant lipid mixing on empty liposomes and increased lipid mixing was seen when Vps1 was added to liposomes population that contained incorporated SNARE proteins (Figure 9b).

Vps1 May Stimulate SNARE-mediated Fusion in a Nucleotide Dependent Manner

In preliminary lipid mixing assays, there was very little difference between the rates of fusion of SNARE proteoliposomes containing Vps1 in the presence of the three nucleotide variants GDP, GTP, and GTγP (Figure 9a). In these assays a lower concentration of SNAREs was used (see Table 3) as well as 10 μM of all nucleotide variants. While SNAREs and Vps1 were both shown to stimulate lipid mixing when compared to controls, there was no discernable difference between the effects of different nucleotides on the reaction.

In later assays, the SNARE protein concertation's were increased to roughly 1:1000 protein to lipid ratios to closer reproduce the functional concentrations being used in many of the recently published intracellular fusion assay (Table 3). The concentration of available nucleotide was also increased from 10 μM to 100 μM in these later assays (Figure 9b,10a,10b). After these modifications, GTP was shown to increase fusion most substantially followed by GDP then GTγP (Figure 9b). In these later assays, the higher concentration of SNARE proteins and nucleotide could account for the increased lipid mixing seen with these samples (Figure 9b&10a).

Endosome-to-TGN SNAREs Alone are not Sufficient to Facilitate Full Fusion and Content Mixing

SNAREs alone showed significantly less lipid mixing when simultaneous reconstitution strategies were used to reconstitute proteoliposomes compared to the previous lipid mixing assays (Figure 10a). This may be due to the difference in reconstitution protocols as the simultaneous assay used a direct methods of SNARE incorporation into preformed liposomes and extended dialysis procedure (Table 9). These differences likely affect membrane permeability as liposomes constructed by the simultaneous method were shown to have almost no content leaking or lysis when test samples were compared with control wells containing unlabeled streptavidin (Figure 10b). As in the previous fusion assays (Figures 8,9a,9b), Vps1 stimulated lipid mixing in the simultaneous assay more than that of SNAREs alone (Figure 10a). Unlike the previous results that found GTP stimulated lipid mixing more than other nucleotides in the presence of Vps1 (Figure 9b), GTγP was shown to most significantly effect lipid mixing in the simultaneous fusion assay. While Vps1 was shown to stimulate lipid mixing in a nucleotide dependent manner, neither SNAREs nor the addition of Vps1 and nucleotide helped to facilitate full fusion and content mixing as no FRET signal between Cy5-Streptavidin and PhycoE-biotin was observed until after TritonX-100 addition and solubilization of the liposomes (Figure 10b). In the simultaneous assay, samples including Dynasore did increase FRET signal, but this is likely due to interference from the fluorescence of Dynasore as this was witnessed in previous trials and the increase in FRET proceeds very slowly which is uncharacteristic of content mixing reactions.

DISCUSSION

SNARE proteins are believed to be key components in regulating membrane fusion, but their exact role in fusion has been extensively debated. This discussion centers on if SNAREs are the minimal fusion machinery that mechanically drives the fusion reaction forward, or if they serve as a scaffold to set up the reaction and allow fusion to progress. The "minimal machinery" hypothesis proposed that cognate *v*- and *t*-SNAREs on apposed membranes are all that is necessary to achieve sufficient membrane fusion at the most basic level (Weber *et al*., 1998). This minimal model has proven inadequate to fully explain fusion as lipid mixing progresses very slow and content mixing is generally minimal or absent. Also, excessively high SNARE concentrations are needed to significantly increase fusion rates, and there have been inconsistency between lipid mixing capabilities when using different intracellular SNARE partners (Nickel *et al*, 1999; Wickner & Rizo, 2017; Furukawa & Mima, 2014). One of the major challenges of interpreting the inconsistencies between reconstitution assays has been the lack of *in vivo* data to support correlations of the numerous *in vitro* models (Chen *et al*, 2006). More recent models of membrane fusion have incorporated a host of other proteins and lipids that hold critical functions in the fusion reaction. While these models still incorporate SNARE pairing and zippering, they also insert many other proteins (such as SMs, tethers, Sec 17/α-SNAP and/or synaptotagmin) directly into the fusion reaction as key component that are just as essential as SNAREs to reconstitute true fusion mechanisms (reviewed in Wickner & Rizo, 2017). In these assays, it was shown that vacuolar fusion had tight requirement for Sec17 binding to assembled SNAREs to further stabilize the complex. Additionally, Sec17 and synaptotagmin-1 were both shown to insert apolar "wedge" domains into the bilayer to facilitate lipid rearrangement that

may cause a local destabilization of the bilayer at fusion "hot spots" in the separate vacuolar and presynaptic membrane fusion models

Homotypic Vacuolar Fusion Model

In yeast, vacuolar fusion models have shown that efficient fusion can be achieved at physiological SNARE levels if Rab/Ypt7 protein was loaded on both membranes in the presence of GTP (Zick & Wickner, 2016). Further studies, have also incorporated requirements for the tether HOPS, which contain the SM protein subunit Vps33 (Baker *et al*, 2015), and fusogenic lipids such as acidic lipids and phosphoinositide's (Stroupe *et al*, 2006; Mima *et al*, 2008; Karunakaran & Wickner, 2013; Orr *et al*, 2015) to recapitulate fusion at physiological SNARE concentrations. Interestingly, Sec17, which is known to function in disassembly, was also shown to bind SNAREs and insert its apolar N-terminal tail domain into the bilayer likely to facilitate lipid rearrangement that may make the bilayers more prone to fuse (Zick *et al*, 2015). Though results from some lipid mixing assays have shown significant lipid dequenching with SNAREs in relatively high concentrations, when SNAREs alone were used in more stringent content mixing assays, very little fusion was detected without the addition of the tether HOPS for vacuolar fusion. (Zick & Wickner, 2013). In addition, high SNARE densities were shown to be accompanied by substantial lysis when measuring content mixing meaning lipid dequenching may likely arise from lysis and reannealing and not traditional fusion mechanisms (Zucchi and Zick, 2011). These findings strongly support the need for a multitude of proteins localized at active zones for fusion to accomplish every stage of the fusion reaction.

Presynaptic Fusion Model

While the involvement of SM proteins in *trans*-SNARE pairing has been extensively studied in presynaptic fusion models, novel roles for additional proteins such as synaptotagmin and functional tethers like Munc13 are still being discovered. While vacuolar and synaptic fusion share common features, the most striking difference is the requirement for Ca^{2+} and the calcium sensor synaptotagmin to trigger neurotransmitter release (Fernandez-Chacon *et al*, 2001). Some other differences that may account for mechanistic deviations are that the Qb and Qc SNARE motifs are actually located on a single SNARE (SNAP-25) and the Qa SNARE (syntaxin-1) adopts a closed conformation that is resistant to *trans*-SNARE assembly (Dulubova *et al*, 1999; Misura *et al*., 2001). It has long been established that the closed conformation of syntaxin-1 strongly associates with the SM protein Munc18 (Dulubova *et al*, 1999), but more recently Munc13's roles in opening syntaxin-1, regulating assembly in a NSF/α-SNAP resistant manner, and vesicle bridging and tethering have been further elucidated (Ma *et al*, 2011; Liu *et al*, 2016). This has led researchers to propose that the multiple functions exhibited by Munc18 and Munc13 in tethering and SNARE assembly may be similar to those fulfilled by the HOPS complex. Though these proteins are very structurally distinct (HOPS is a five-subunit complex), their differences may allow for the multiple modes of regulation necessary for presynaptic membrane fusion (Wickner & Rizo, 2017). As is the case for reconstituted vacuolar fusion, high densities of neuronal SNAREs alone were needed to facilitate fusion. This likely means that the integrity of the membrane was compromised as judged by substantial leakage and PEG was again necessary to induce tethering (Dennison *et al*, 2006). Later it was found that the addition of synaptotagmin-1 and Ca^{2+} could induce content mixing at near physiological SNARE concentration (Lai *et al*, 2013). More recent membrane reconstitutions containing Munc18-1, Munc13-1, NSF, α-SNAP,

and the neuronal SNAREs showed that these proteins assembled and formed a primed state that could readily induce lipid mixing, but little content mixing was observed without the addition of Ca^{2+} in the presence of synaptotagmin-1 (Liu *et al*, 2016). These findings, as well as those in the vacuolar system, support the assertion that SNAREs alone are not sufficient to complete the full fusion reaction cycle.

Endosome-to-Golgi Fusion Model

Numerous fusion assays have been performed in the vacuolar and presynaptic systems, but assays reconstituting endosomal fusion are seriously lacking. To date, only two published lipid mixing assay have been employed incorporating the same endo-to-TGN yeast SNAREs used in this study; Snc2p, Tlg2p, Tlg1p, and Vti1p (Paumet *et al*, 2001; Paumet *et al*, 2004). Interestingly, in the previous research almost no lipid mixing was observed without the activation of the syntaxin Qa-SNARE (Tlg2p) by a 33-amino acid Snc2 C-terminal peptide. Our data supports their previous findings that little to no lipid mixing happens in the presence of SNAREs alone, but we were unable to induce fusion using this Snc2 C-terminal peptide. Even using concentrations as high as 1 mM and following the preincubation strategies suggested to enhance the reaction rate I was unable to increase the rate of fusion more than that of SNAREs alone. This could possibly be due to the differences in construction since the peptide used by Paumet *et al*, 2001 was purified as a recombinant protein and our peptide was constructed by synthesis. It is possible that our synthetic peptide was unable to adopt a functional secondary structure, although structural data to elucidate the specific mechanism by which this peptide activates the syntaxin was not included in the previous studies (Paumet *et al*, 2001; Paumet *et al*, 2004).

Related Finding of this Study

In a systematic lipid mixing study assessing the fusogenisity of liposomes containing variable *v* and *t*-SNARE arrangements of 14 purified yeast SNAREs involved in ER-to-Golgi, intraGolgi, endosomal, and vacuolar fusion; a requirement for tethering factors was necessary for endosomal and ER-Golgi SNAREs to achieve substantial lipid mixing. In those assays, endosomal fusion was enhanced by PEG-mediated synthetic tethering, while ER-Golgi fusion required PEG-mediated tethering as well as the addition of the resident SM protein Sly1p (Furukawa & Mima, 2014). The SNAREs partners used in this work were very similar to the endosomal SNAREs used in the systematic study. The only difference in the cognate SNARE pairings being used was that the syntaxin Qa-SNAREs in this study was Tlg2p to represent endo-Golgi fusion, while Furukawa and Mima, 2014 used Pep12 as the Qa-SNARE to mimic endosomal fusion. In fact, all other SNAREs used in this study (Snc2, Tlg1, and Vti1) were generously donated by Dr. Mima's lab and were purified from the same plasmid constructs as those used in their published work (Furukawa & Mima, 2014). While the syntaxin's are different, which may result in considerably different mechanism of activation, findings from my study are consistent with their findings that SNAREs alone are not sufficient to facilitate significant lipid mixing. Their research did find that endosomal lipid mixing could be stimulated by PEG-mediated tethering, which may also be the case for endosome-to-TGN fusion.

Vps1's Role in Membrane Fusion

The fusion assays used in my study to characterize endo-to-TGN membrane fusion are the first to incorporate the dynamin-like protein Vps1 into multiple reconstituted *in vitro* fusion assays. My research is also the first to study Vps1's involvement in SNARE-mediated

endosome-to-TGN fusion. In previous studies, Vps1 was proposed to facilitate vacuolar *trans*-SNARE assembly through sequestration of Qa-SNARE (Vam3) and facilitating Vam3's interaction with HOPS complex (Alpadi *et al*, 2013). Later research from the same lab also asserted a role for Vps1 in the transition from hemifusion to content mixing in homotypic vacuolar fusion through oligomerization of Vps1 and binding the SNARE domain of Vam3 to increase the number of available *trans*-SNAREs for fusion (Kulkarni *et al*, 2014). While findings from these two papers have provided novel insight supporting a role for Vps1 in vacuolar fusion there have been no follow up studies to support these initial observations. Furthermore, an abundance of yeast vacuolar fusion assays have been conducted with both purified yeast vacuole and liposomes containing purified SNAREs (see Introduction and earlier Discussion) and none of these experiments required Vps1 to recapitulate fusion. While my research does support a nucleotide dependent role for Vps1 in lipid mixing and possible hemifusion, my results do not support a model in which SNAREs and Vps1 alone can facilitate full fusion and content mixing. One major difference that may account for the discrepancy in the results is that my assay did not incorporate tethering factors such as HOPS, which was used both in the Alpadi *et al*, 2013 and Kulkarni *et al*, 2014 assays. In addition, HOPS holds dual functions in tethering and SNARE assembly as the SM protein (Vps33) is incorporated into the 5 subunit complex and it has been extensively shown that HOPS facilitates both lipid and content mixing, as mentioned previously. One other possible explanations for this discrepancy is that previous research in our lab found no interaction between Vps1 and any of the endo-TGN SNAREs used in the reconstitutions as judged by GST-pulldown, though a previous Yeast-2-Hybrid assay provided evidence of interactions between Vps1 and endo-TGN SNAREs Snc2 and Vti1 (Makaraci *et al*, 2018). It is possible that Vps1 tethers liposomal membranes by a mechanism that requires nucleotide

dependent oligomerization but does not associate or has weak association with SNARE proteins during tethering which is illustrated and discussed in the working model for Vps1 assisted endosome-to-Golgi fusion (Figure 11). As all reconstitutions using endo-to-TGN SNAREs alone have failed to recapitulate fusion without additional factors (Snc2-C-Pept or PEG-mediated tethering), it is likely that the addition of tethering factors such as GARP or PEG-mediation may help to facilitate lipid and/or content mixing.

Future Directions

While my data strongly support the role of Vps1 in increasing SNARE-mediated lipid mixing, the fusion reaction was relatively slow and no content mixing was observable in any of the experimental conditions. Furthermore, my research only represents initial pilot studies to evaluate the efficiency of reconstitution techniques and assess general trends in the data to facilitate future studies for the role of Vps1 in fusion. These future studies should increase the sample size to include the average of three separate trials (n=3) with three technical replicates for each sample condition being studied. Further studies should also incorporate the additional protein factors shown to be necessary in both vacuolar and synaptic membrane fusion, mainly tethers with associated Rab's and SM-like proteins. Of these factors, tethering can be artificially simulated using PEG solution as previously mentioned or by the addition of the Golgi tethering factor GARP. The relevant endosome-to-Golgi SM protein (Vps45) may also be required for activation of the Qa-SNARE (Tlg2) and/or *trans*-SNARE assembly, so preincubation of liposomes with Vps45 may facilitate faster lipid and/or content mixing. Lastly, the lipid compositions of the reconstituted liposomes can be further marked for specificity using PI3P and PI4P on *v*- and *t*-liposomes to better mimic endosomal and Golgi membranes, respectively.

REFERENCES

Alpadi K, Kulkarni A, Namjoshi S, Srinivasan S, Sippel K, Ayscough K, Zieger M, Schmidt A, Mayer A, Evangelista M, Quiocho F & Peters C (2013) Dynamin−SNARE interactions control trans-SNARE formation in intracellular membrane fusion. *Nature Communications* 4: 1704

Baker R & Hughson F (2016) Chaperoning SNARE assembly and disassembly. *Nature Reviews Molecular Cell Biology* 17: 465-479

Baker R, Jeffrey P, Zick M, Phillips B, Wickner W & Hughson F (2015) A direct role for the Sec1/Munc18-family protein Vps33 as a template for SNARE assembly. *Science* 349: 1111-1114

Barr F (2013) Rab GTPases and membrane identity: Causal or inconsequential?. *The Journal of Cell Biology* 202: 191-199

Brocker C, Kuhlee A, Gatsogiannis C, kleine Balderhaar H, Honscher C, Engelbrecht-Vandre S, Ungermann C & Raunser S (2012) Molecular architecture of the multisubunit homotypic fusion and vacuole protein sorting (HOPS) tethering complex. *Proceedings of the National Academy of Sciences* 109: 1991-1996

Burkhardt P, Hattendorf D, Weis W & Fasshauer D (2008) Munc18a controls SNARE assembly through its interaction with the syntaxin N-peptide. *The EMBO Journal* 27: 923-933

Chen X, Araç D, Wang T, Gilpin C, Zimmerberg J & Rizo J (2006) SNARE-Mediated Lipid Mixing Depends on the Physical State of the Vesicles. *Biophysical Journal* 90: 2062-2074

Chernomordik L & Kozlov M (2008) Mechanics of membrane fusion. *Nature Structural & Molecular Biology* 15: 675-683

Dawidowski D & Cafiso D (2016) Munc18-1 and the Syntaxin-1 N Terminus Regulate Open-Closed States in a t-SNARE Complex. *Structure* 24: 392-400

Demircioglu F, Burkhardt P & Fasshauer D (2014) The SM protein Sly1 accelerates assembly of the ER-Golgi SNARE complex. *Proceedings of the National Academy of Sciences* 111: 13828-13833

Dennison S, Bowen M, Brunger A, & Lentz B (2006). Neuronal SNAREs Do Not Trigger Fusion between Synthetic Membranes but Do Promote PEG-Mediated Membrane Fusion. *Biophysical Journal* 90: 1661-1675

Dulubova I, Sugita S, Hill S, Hosaka M, Fernandez I, Südhof T & Rizo J (1999) A conformational switch in syntaxin during exocytosis: role of munc18. *The EMBO Journal* 18: 4372–4382

Dulubova I, Yamaguchi T, Gao Y, Min S, Huryeva I, Südhof T & Rizo J (2002) How Tlg2p/syntaxin 16 snares Vps45. *The EMBO Journal* 21: 3620–3631

Fasshauer D, Sutton R, Brunger A & Jahn R (1998) Conserved structural features of the synaptic fusion complex: SNARE proteins reclassified as Q- and R-SNAREs. *Proceedings of the National Academy of Sciences* 95: 15781-15786

Fernández-Chacón R, Königstorfer A, Gerber S, García J, Matos M, Stevens C, Brose N, Rizo J, Rosenmund C & Südhof T (2001) Synaptotagmin I functions as a calcium regulator of release probability. *Nature* 410: 41-49

Fratti R, Jun Y, Merz A, Margolis N & Wickner W (2004) Interdependent assembly of specific regulatory lipids and membrane fusion proteins into the vertex ring domain of docked vacuoles. *The Journal of Cell Biology* 167: 1087-1098

Furgason M, MacDonald C, Shanks S, Ryder S, Bryant N & Munson M (2009) The N-terminal peptide of the syntaxin Tlg2p modulates binding of its closed conformation to Vps45p. *Proceedings of the National Academy of Sciences* 106: 14303-14308

Furukawa N & Mima J (2014) Multiple and distinct strategies of yeast SNAREs to confer the specificity of membrane fusion. *Scientific Reports* 4: 4277

Giraudo C, Hu C, You D, Slovic A, Mosharov E, Sulzer D, Melia T & Rothman J (2005) SNAREs can promote complete fusion and hemifusion as alternative outcomes. *The Journal of Cell Biology* 170: 249–260

Gundersen C (2017) The Structure of the Synaptic Vesicle-Plasma Membrane Interface Constrains SNARE Models of Rapid, Synchronous Exocytosis at Nerve Terminals. *Frontiers in Molecular Neuroscience* 10: 48

Han J, Pluhackova K & Böckmann R (2017) The Multifaceted Role of SNARE Proteins in Membrane Fusion. *Frontiers in Physiology* 8: 5

Karunakaran V & Wickner W (2013) Fusion proteins and select lipids cooperate as membrane receptors for the solubleN-ethylmaleimide-sensitive factor attachment protein receptor (SNARE) Vam7p. *Journal of Biological Chemistry* 288: 31914-31914

Kloepper T, Kienle C & Fasshauer D (2007) An Elaborate Classification of SNARE Proteins Sheds Light on the Conservation of the Eukaryotic Endomembrane System. *Molecular Biology of the Cell* 18: 3463-3471

Kulkarni A, Alpadi K, Sirupangi T & Peters C (2014) A Dynamin Homolog Promotes the Transition from Hemifusion to Content Mixing in Intracellular Membrane Fusion. *Traffic* 15: 558-571

Kümmel D & Ungermann C (2014) Principles of membrane tethering and fusion in endosome and lysosome biogenesis. *Current Opinion in Cell Biology* 29: 61-66

Lai Y, Diao J, Liu Y, Ishitsuka Y, Su Z, Schulten K, Ha T & Shin Y (2013) Fusion pore formation and expansion induced by Ca2+and synaptotagmin 1. *Proceedings of the National Academy of Sciences* 110: 1333-1338

Lee S, Kovacs J, Stahelin R, Cheever M, Overduin M, Setty T, Burd C, Cho W & Kutateladze T (2006) Molecular Mechanism of Membrane Docking by the Vam7p PX Domain. *Journal of Biological Chemistry* 281: 37091-37101

Liu X, Seven A, Camacho M, Esser V, Xu J, Trimbuch T, Quade B, Su L, Ma C, Rosenmund C & Rizo J (2016) Functional synergy between the Munc13 C-terminal C1 and C2 domains. *eLife* 5: 13696

Liu X, Seven A, Xu J, Esser V, Su L, Ma C & Rizo J (2017) Simultaneous lipid and content mixing assays for in vitro reconstitution studies of synaptic vesicle fusion. *Nature Protocols*12: 2014-2028

Lürick A, Gao J, Kuhlee A, Yavavli E, Langemeyer L, Perz A, Raunser S & Ungermann C (2017) Multivalent Rab interactions determine tether-mediated membrane fusion. *Molecular Biology of the Cell* 28: 322–332

Ma C, Li W, Xu Y, Rizo J (2011) Munc13 mediates the transition from the syntaxin-Munc18 complex to the SNARE complex. *Nature Structural Mollecular Biology* 18: 542–549

MacDonald C, Munson M & Bryant N (2010) Autoinhibition of SNARE complex assembly by a conformational switch represents a conserved feature of syntaxins. *Biochemical Society Transactions* 38: 209-212

Makaraci P, Cruz M, McDermott H, Nguyen V, Highfill C & Kim K (2018) Yeast dynamin and Ypt6 function in parallel for the endosome-to-Golgi retrieval of Snc1. *Cell Biology International* 110:42

Malia P & Ungermann C (2016) Vacuole membrane contact sites and domains: emerging hubs to coordinate organelle function with cellular metabolism. *Biochemical Society Transactions* 44: 528-533

Martens S & McMahon H (2008) Mechanisms of membrane fusion: disparate players and common principles. *Nature Reviews Molecular Cell Biology* 9: 543-556

Mima J, Hickey C, Xu H, Jun Y & Wickner W (2008) Reconstituted membrane fusion requires regulatory lipids, SNAREs and synergistic SNARE chaperones. *The EMBO Journal* 27: 2031-2042

Misura K, Scheller R & Weis W (2001) Self-Association of The H3 Region Of Syntaxin 1A: Implications For Snare Complex Assembly. *The Journal of Biological Chemistry* 16: 13273–13282

Nickel W, Weber T, McNew J, Parlati F, Sollner T & Rothman J (1999) Content mixing and membrane integrity during membrane fusion driven by pairing of isolated v-SNAREs and t-SNAREs. *Proceedings of the National Academy of Sciences* 96: 12571-12576

Orr A, Wickner W, Rusin S, Kettenbach A & Zick M (2015) Yeast vacuolar HOPS, regulated by its kinase, exploits affinities for acidic lipids and Rab:GTP for membrane binding and to catalyze tethering and fusion. *Molecular Biology of the Cell* 26: 305-315

Paumet F, Brügger B, Parlati F, McNew J, Söllner T & Rothman J (2001) A t-SNARE of the endocytic pathway must be activated for fusion. *The Journal of Cell Biology* 155: 961-968

Paumet F, Rahimian V & Rothman J (2004) The specificity of SNARE-dependent fusion is encoded in the SNARE motif. *Proceedings of the National Academy of Sciences* 101: 3376-3380

Peters C, Baars T, Bühler S & Mayer A (2004) Mutual Control of Membrane Fission and Fusion Proteins. *Cell* 119: 667-678

Progida C & Bakke O (2016) Bidirectional traffic between the Golgi and the endosomes – machineries and regulation. *Journal of Cell Science* 21: 3971-3982

Rizo J & Xu J (2015) The Synaptic Vesicle Release Machinery. *Annual Review of Biophysics* 44: 339-367

Saimani U, Smothers J, McDermott H, Makaraci P & Kim K (2017) Yeast dynamin associates with the GARP tethering complex for endosome-to-Golgi traffic. *European Journal of Cell Biology* 96: 612-621

Smolarsky M, Teitelbaum D, Sela M & Gitler C (1977) A simple fluorescent method to determine complement-mediated liposome immune lysis. *Journal of Immunological Methods* 15: 255-265

Söllner T, Bennett M, Whiteheart S, Scheller R & Rothman J (1993) A protein assembly-disassembly pathway in vitro that may correspond to sequential steps of synaptic vesicle docking, activation, and fusion. Cell 75: 409–418

Stroupe C, Collins K, Fratti R & Wickner W (2006) Purification of active HOPS complex reveals its affinities for phosphoinositides and the SNARE Vam7p. *The EMBO Journal* 25: 1579-1589

Südhof T & Rizo J (2011) Synaptic Vesicle Exocytosis. *Cold Spring Harbor Perspectives in Biology* 3: 5637

Südhof T & Rothman J (2009) Membrane Fusion: Grappling with SNARE and SM Proteins. *Science* 323: 474-477

Südhof T (2013a) A molecular machine for neurotransmitter release: synaptotagmin and beyond. *Nature Medicine* 19: 1227-1231

Südhof T (2013b) Neurotransmitter Release: The Last Millisecond in the Life of a Synaptic Vesicle. *Neuron* 80: 675-690

Südhof T (2014) The Molecular Machinery of Neurotransmitter Release (Nobel Lecture). *Angewandte Chemie International Edition* 53: 12696-12717

Varlakhanova N, Alvarez F, Brady T, Tornabene B, Hosford C, Chappie J, Zhang P & Ford M (2018) Structures of the fungal dynamin-related protein Vps1 reveal a unique, open helical architecture. *The Journal of Cell Biology* 217: 3608-3624

Weber T, Zemelman B, Mcnew J, Westermann B, Gmachl M, Parlati F, Söllner T & Rothman J (1998) SNAREpins: Minimal Machinery for Membrane Fusion. *Cell* 92**:** 759–772

Wickner W & Schekman R (2008) Membrane fusion. *Nature Structural & Molecular Biology* 15: 658-664

Wickner W & Rizo J (2017) A cascade of multiple proteins and lipids catalyzes membrane fusion. *Molecular Biology of the Cell* 28: 707-711

Zick M, Stroupe C, Orr A, Douville D & Wickner W (2014) Membranes linked by trans-SNARE complexes require lipids prone to non-bilayer structure for progression to fusion. eLife 3: e01879

Zick M & Wickner W (2013) The tethering complex HOPS catalyzes assembly of the soluble SNARE Vam7 into fusogenic trans-SNARE complexes. *Molecular Biology of the Cell* 24: 3746–3753

Zick M & Wickner W (2016) Improved reconstitution of yeast vacuole fusion with physiological SNARE concentrations reveals an asymmetric Rab(GTP) requirement. *Molecular Biology of the Cell* 27: 2590-2597

Zucchi P & Zick M (2011) Membrane fusion catalyzed by a Rab, SNAREs, and SNARE chaperones is accompanied by enhanced permeability to small molecules and by lysis. *Molecular Biology of the Cell* 22: 4635-4646

Table 1: Yeast and mammalian SNARE and SM proteins for each type of fusion being discussed

Presynaptic/Plasma Membrane Fusion

Fusion Proteins	Yeast	Mammalian
v-SNARE	Snc1/2	Synaptobrevin
t-SNARE	Sso1/2, Sec9	Syntaxin1, SNAP-25,
SM-like protein	Sec1	MUNC-18

Homotypic Vacuolar Fusion

Fusion Proteins	Yeast	Mammalian
v-SNARE	Nyv1	VAMP8?
t-SNARE	Vam3, Vti1, Vam7	Syntaxin7, VTI1b, Syntaxin8?
SM-like protein	Vps33	VPS33a/b

Endosome-to-Golgi Fusion

Fusion Proteins	Yeast	Mammalian
v-SNARE	Snc2	VAMP-4
t-SNARE	Tlg2, Vti1, Tlg1	Syntaxin16, VTI1a, Syntaxin6
SM-like protein	Vps45	VPS45

Table 2: Lipid concentrations used for lipid mixing assay

Premixed lipids for Lipid Mixing Assay (6 mM)				
Lipid Stocks	**Mol%**	**_v_-SNARE lipids**	**Mol%**	**_t_-SNARE lipids**
DOPC 18:1 (25 mg/mL)	82	30.94 µL	85	80.18 µL
DOPS 18:1 (10 mg/mL)	15	14.58 µL	15	36.45 µL
NBD-PE 18:1 (1 mg/mL)	1.5	16.63 µL	-	-
Liss Rhod-PE (1 mg/mL)	1.5	23.43 µL	-	-
Chloroform (200 µL total)	-	114.41 µL	-	83.37 µL

Table 3: SNARE protein concentrations for lipid mixing assay

v-SNARE Liposomes				
v-SNAREs	**[Molar]**	**Initial Trials Volumes**	**[Molar]**	**Final Assays Volumes**
Snc2p (84.88 μM)	40 nM	0.188 μL	6 μM	28.28 μL
Reconstitution Buffer w/ 1% βOG	-	399.81 μL	-	371.72 μL
t-SNARE Liposomes				
t-SNAREs	**[Molar]**	**Initial Trials**	**[Molar]**	**Final Assays**
Tlg2p (27.83 μM)	40 nM	0.92 μL	2 μM	46 μL
Tlg1p (12.3 μM)	40 nM	2.3 μL	2 μM	115 μL
Vti1p (13.25 μM)	40 nM	2.92 μL	2 μM	146 μL
Reconstitution Buffer w/ 1% βOG	-	993.86 μL	-	693 μL

Table 4. Well contents of 96-well plates for lipid mixing assay and simultaneous fusion assays

Contents of each well of 96-well plate

	1	2	3	4	5	6	7	8	9	10
Lane	+ v-lipo	+ v-lipo	+ v-lipo	+ v-lipo	+ v-lipo	+ v-	+ v-lipo	+ v-lipo	+ v-lipo	+ v-lipo
	+t-lipo	+t-lipo	+t-lipo	+t-lipo	+t-lipo	lipo	+t-lipo	+t-lipo	+Buffer	+ Buffer
A		+Snc2-	+Snc2-	+Vps1	+Vps1	+t-lipo	+Vps1	+Vps1		+Vps1
		C-pept	C-pept		+GTP	+Vps1	+GTγ -P	+GTP		+GTP
			+Vps1		+Dynasore	+GDP				
			+GTP							

Table 5: Lipid concentrations for simultaneous lipid and content mixing assay

Premixed Lipids for Simultaneous Fusion Assay (5 mM)						
Lipid Stocks	Mol%	*v*-liposome for lipid mixing	Mol%	*v*-liposomes for content mixing	Mol%	*t*-liposomes used for both
DOPC 18:1 (25 mg/mL)	39	25.76 μL	40	26.42 μL	40	26.42 μL
DOPS 18:1 (10 mg/mL)	19	32.32 μL	20	34.02 μL	20	34.02 μL
DOPE 18:1 (10 mg/mL)	19	29.69 μL	20	31.25 μL	20	31.25 μL
Ergosterol (10 mg/mL)	20	16.66 μL	20	16.66 μL	20	16.66 μL
NBD-PE 18:1 (1 mg/mL)	1.5	29.11 μL	-	-	-	-
Liss Rhod-PE (1 mg/mL)	1.5	41.01 μL	-	-	-	-

Table 6: Protein and lipid concentrations used to reconstitute *v*-liposome for simultaneous assay

v-SNAREs	Final Concentration	Lipid mixing volume	Final Concentration	Content mixing volume
v-SNARE Liposomes (500 µL)				
Snc2p (84.88 µM)	5 µM	29.45 µL	5 µM	29.45 µL
Reconstitution Buffer	Containing 1% βOG	100 µL	Containing 1% βOG	100 µL
Premixed lipids for Lipid/Content (5 mM)	2 mM	200 µL	2 mM	200 µL
Reconstitution Buffer	Containing 1% βOG	170.55 µL	-	-
Cy5-Streptavidin (16 µM) w/ 1% βOG	-	-	~5.5 µM	170.55 µL

Table 7: Concentration of t-SNAREs for overnight incubation for assembly of *trans* complex's

t-SNAREs	Final Molar concentrations	Volumes of SNAREs (x2 for content & lipid mixing assays)
t-SNARE Incubation (4 ˚C)		
Tlg2p (27.83 µM)	1 µM	53.9 µL
Tlg1p (12.3 µM)	1 µM	89.32 µL
Vti1p (13.25µM)	1 µM	113.2 µL
Reconstitution Buffer	-	92 µL

Table 8: Protein and lipid concentrations used to reconstitute t-liposome for simultaneous assay

t-SNARE Liposomes (500 µL)				
v-SNAREs	Final Concentration	Lipid mixing volume	Final Concentration	Content mixing volume
Assembled *t*-SNAREs	Incubated w/ 1% βOG	174.2 µL	Incubated w/ 1% βOG	174.2 µL
Premixed lipids for *t*-liposomes (5 mM)	2 mM	200 µL	2 mM	200 µL
20% βOG	~1%	6 µL	~1%	6 µL
Reconstitution Buffer	1% βOG	119.8 µL	-	-
PychoE-Biotin (16.7 µM) w/ 1% βOG	-	-	4 µM	119.8 µL

Table 9: Dialysis times and conditions for simultaneous fusion assay

	Buffer Volume	SM-2 Bead	Time	Temperature
Simultaneous Assay Dialysis				
1st run	0.5 L	1 g	1hr	Room temp.
2nd run	0.5 L	1 g	2hr	4 ℃
Final run	1 L	2 g	~16hr	4 ℃

Table 10: Electroformation conditions using function generator

Steps	Vpp	Frequency (Hz)	Time
Pt-wire GUV Electroformation			
1	1 → 2 V	300	1hr
2	2 V	300	2hr
3	2 V	50 → 2	30min, 30min
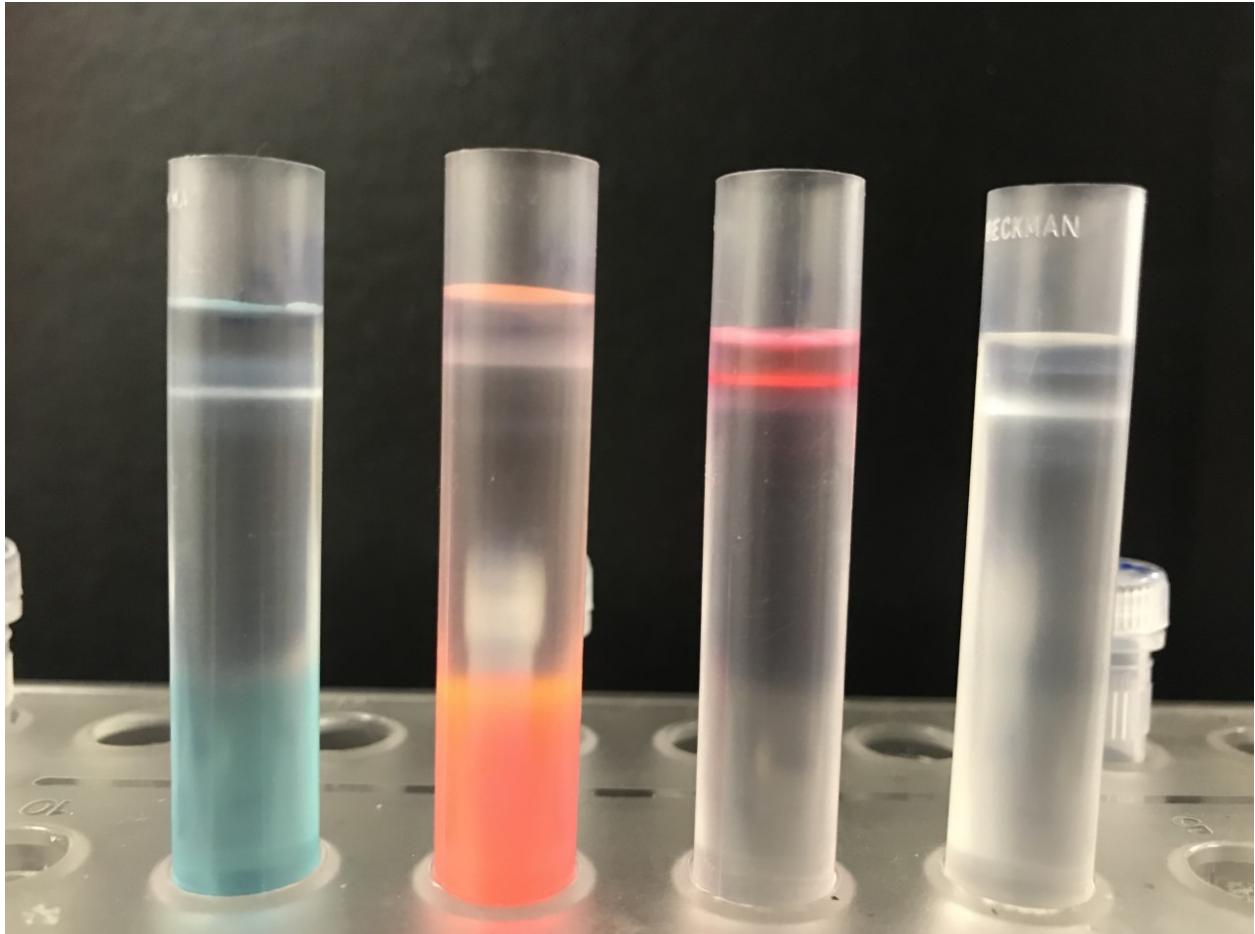
Figure 1: Liposome separations after ultracentrifugation with Nycodenz floatation gradient. The simultaneous fusion assay has the advantage of making vesicle separation layers clearly visible due to the used of multiple fluorescent molecules. The florescent content and assay used for each of the liposomes are in ordered from left to right as shown; Cy5-Streptavidin incorporated into *t*-liposomes for the content mixing, PhycoE-biotin incorporated into *v*-liposomes for content mixing, Liss-Rhodamine PE lipids (quenching NBD-PE) used to reconstitute *v*-liposomes for lipid mixing. No florescent labels were used to create *t*-liposomes for the lipid mixing assay (far right) as mixing is measured by the dequenching of NBD florescence from Liss-Rhodamine upon fluorophore dilution on unlabeled membranes.
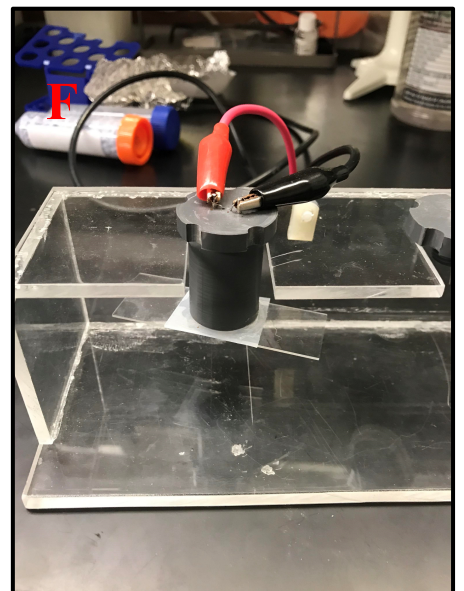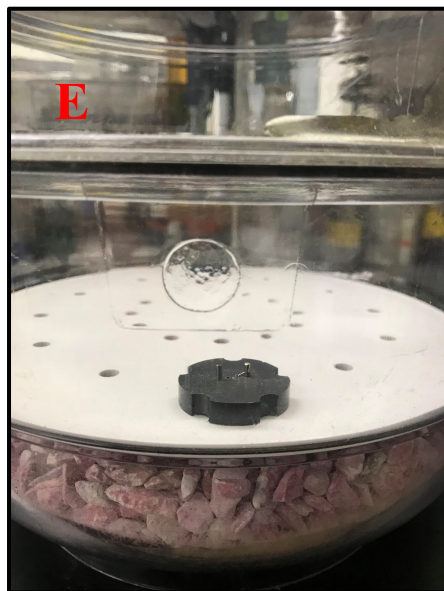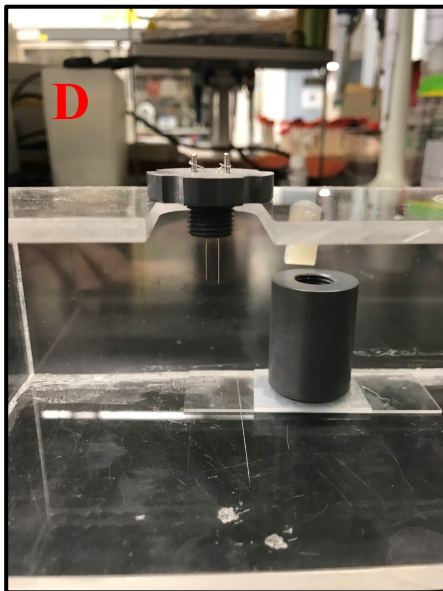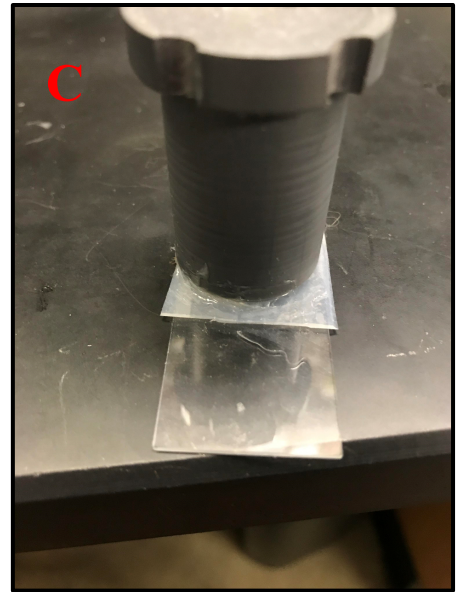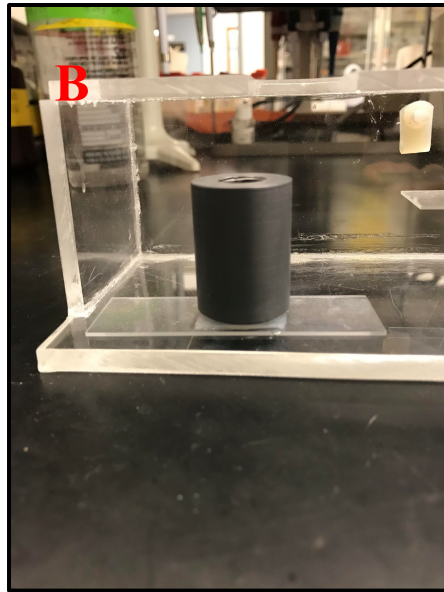
Figure 2. Pt-wire electroformation chamber assembly procedures. The electroformation chamber was assembled as discussed in the Methods section.
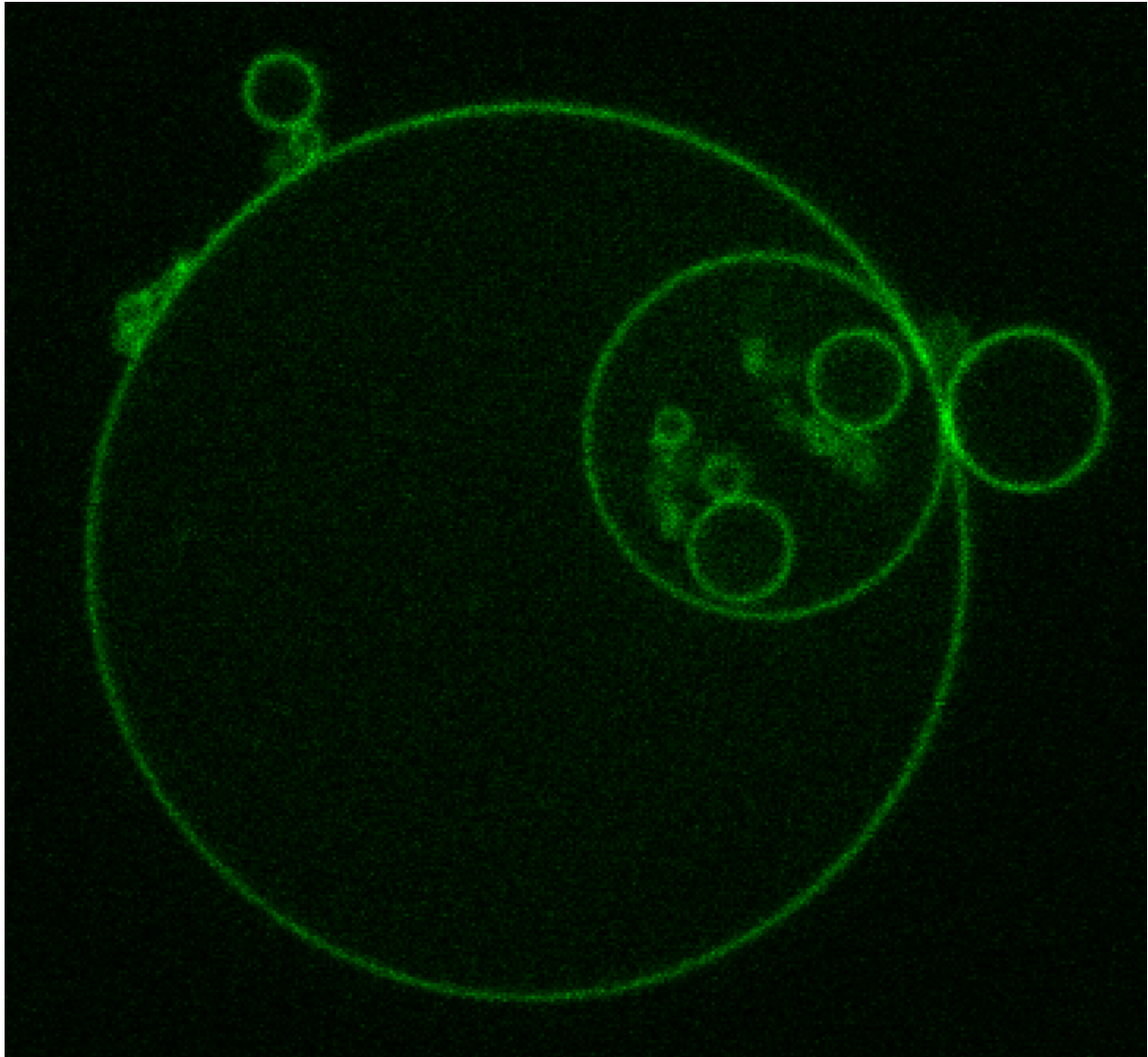
Figure 3: Picture of GUVs formed by electroformation on Pt-wire. The GUV's were formed by electroformation on Pt-wire and visualized using confocal microscopy as discussed in the Methods section.
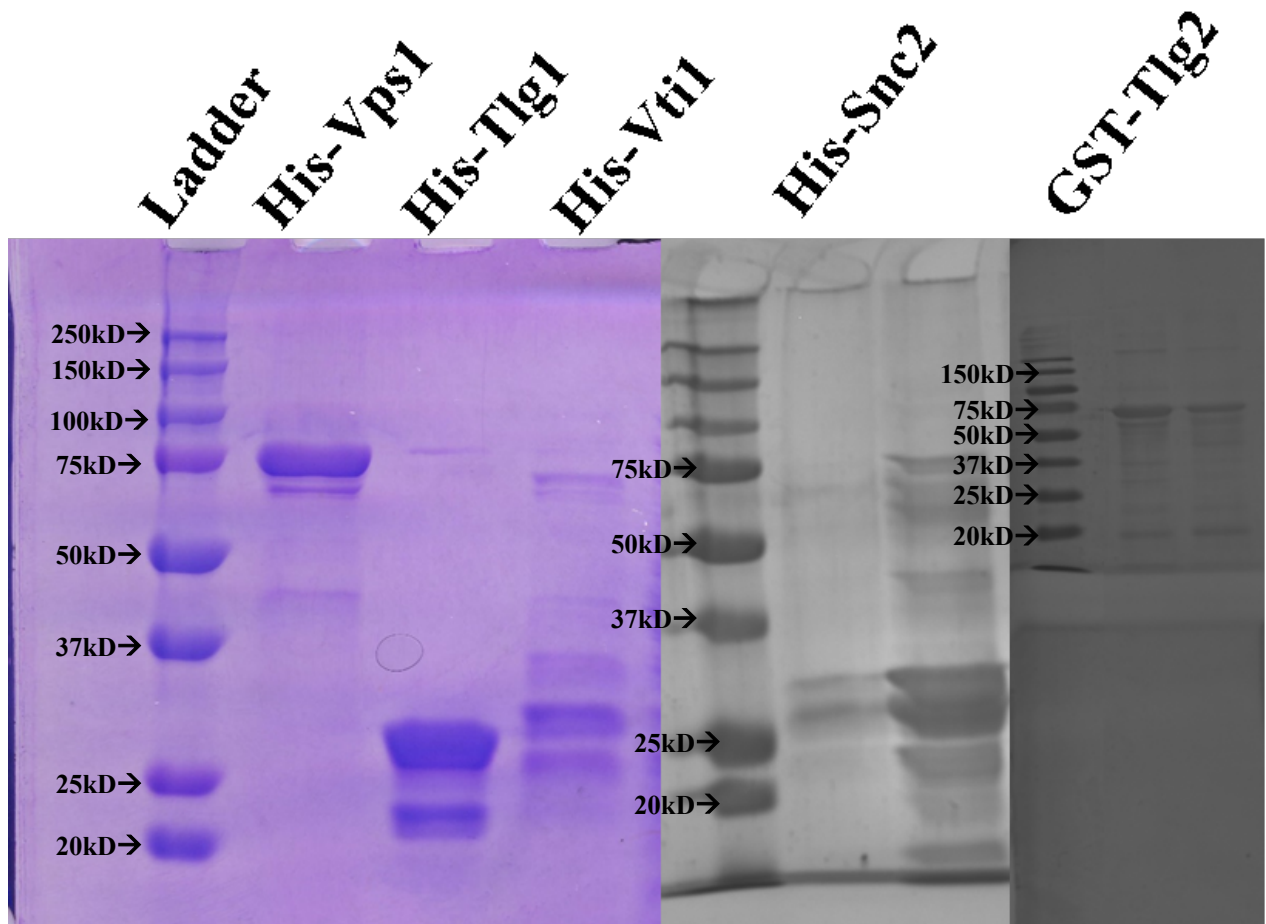
Figure 4: Yeast endo-to-Golgi fusion protein used in this study. Proteins were visualized after Coomassie blue staining using and HP laser jet scanner (purple images) or with an Azure C-series advanced imaging system (black and white images). Proteins from left to right are as follows; His-Vps1p (79 kDa), His-Tlgp1 (26.5 kDa), His-Vti1p (26.5 kDa), His-Snc2 (24 kDa), GST-Tlg2p (70 kDa)
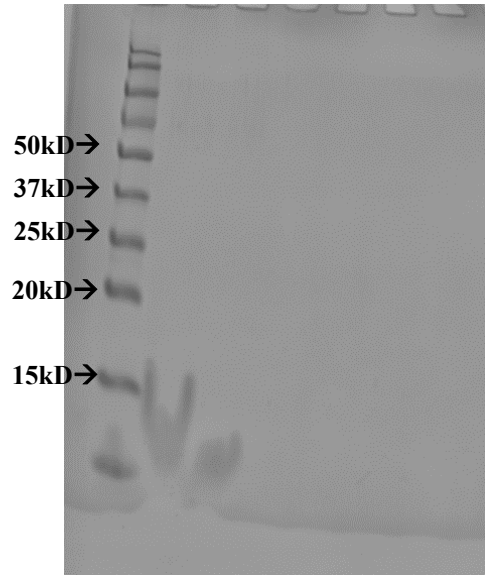
Figure 5: Confirmation of *v*-SNARE incorporation into proteoliposomes. *V*-liposomes were solubilized in 1xPBS containing SDS and the proteins incorporated into the proteoliposome were separated using SDS-PAGE gel electrophoresis. Western blot analysis and anti-His antibodies were used to confirm the presences of His-Snc2p (14kD after cleavage). The smearing is likely due to lipid contaminations from the liposomes, which should be previously solubilized with 1% Triton X-100 before protein clarification by centrifugation.
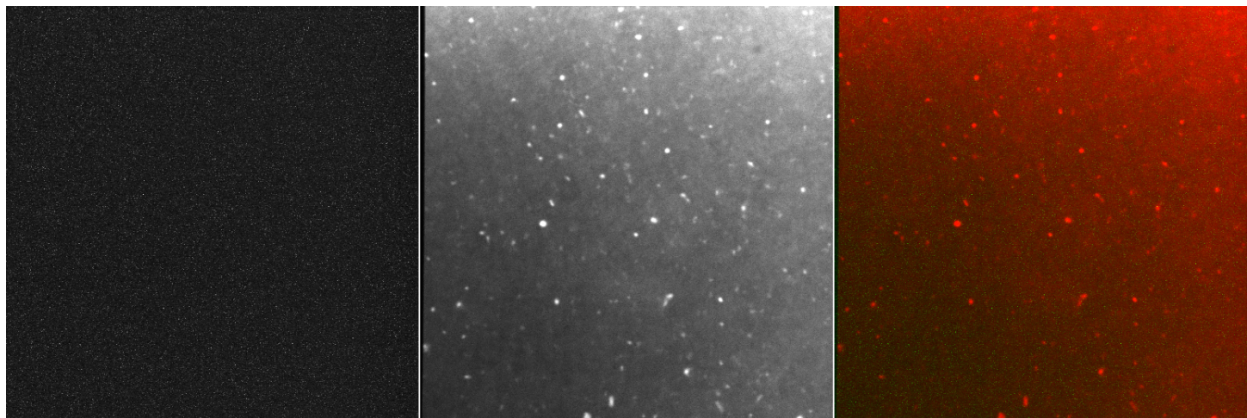
Figure 6: Visualization of liposome formation with confocal microscopy. Liposomes were loaded into wells prepared on glass slides and visualize using confocal microscopy with simultaneous RFP and GFP excitation and emissions. The above figure shows the multi-view of each wavelength from left to right; GFP, RFP, both GFP and RFP. Liposomes should only be visible when excited with RFP lasers as Liss Rhodamine-PE will quench the emission of NBD-PE excited by GFP wavelengths. See figure 3 for an example of GUV's prepared with NBD-PE alone and visualized using GFP wavelengths.
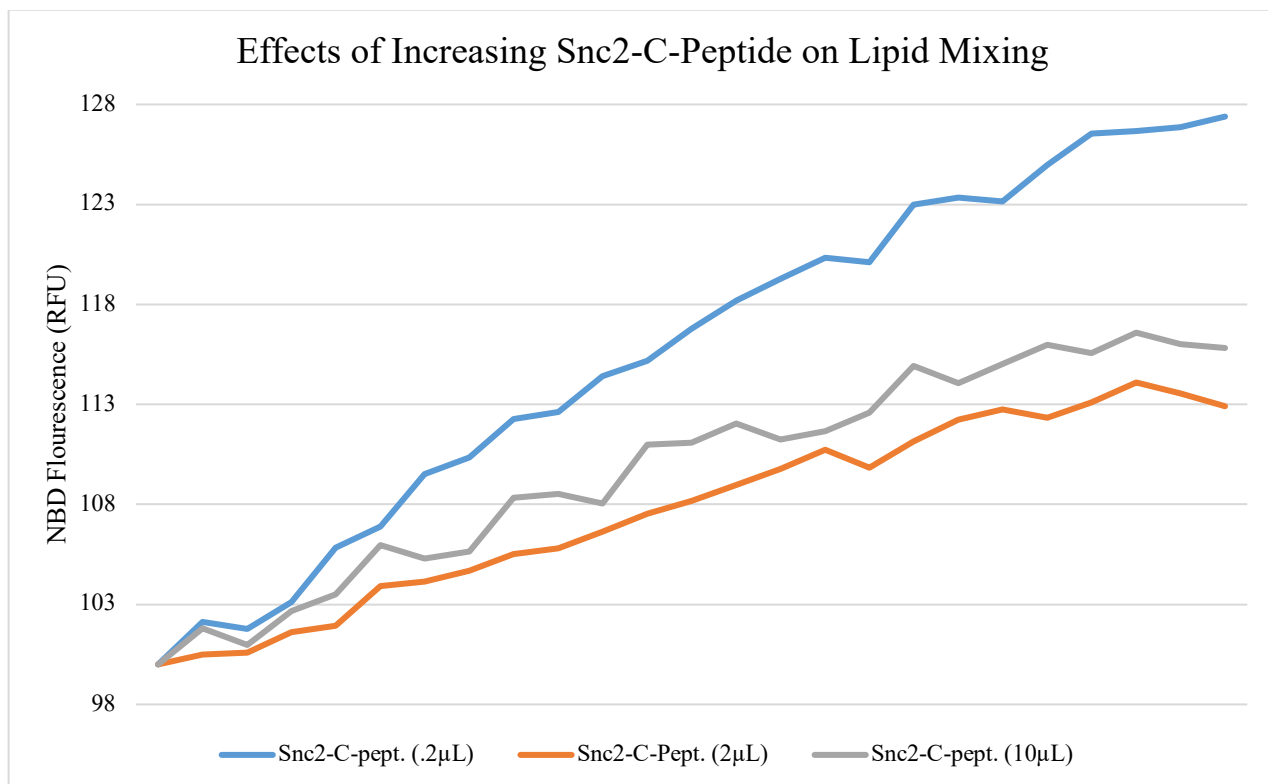
Figure 7: Effects of increasing Snc2-C-terminal peptide concentrations on endo-to-TGN liposome fusion. Proteoliposomes for lipid mixing were prepared as described in the methods with the protein concentration used for "Initial Trial Volumes" (Table 3). All wells were prepared with 5 µL v-liposomes and 45 µL t-liposome and incubated with above concentrations of Snc2-C-terminal peptide for 2 hours at 4 ℃ before the fusion reaction was started. Lipid mixing assays were monitored by dequenching of NBD-PE from Liss Rhod-PE (excitation 460nm emission 538 nm) for 2 hours
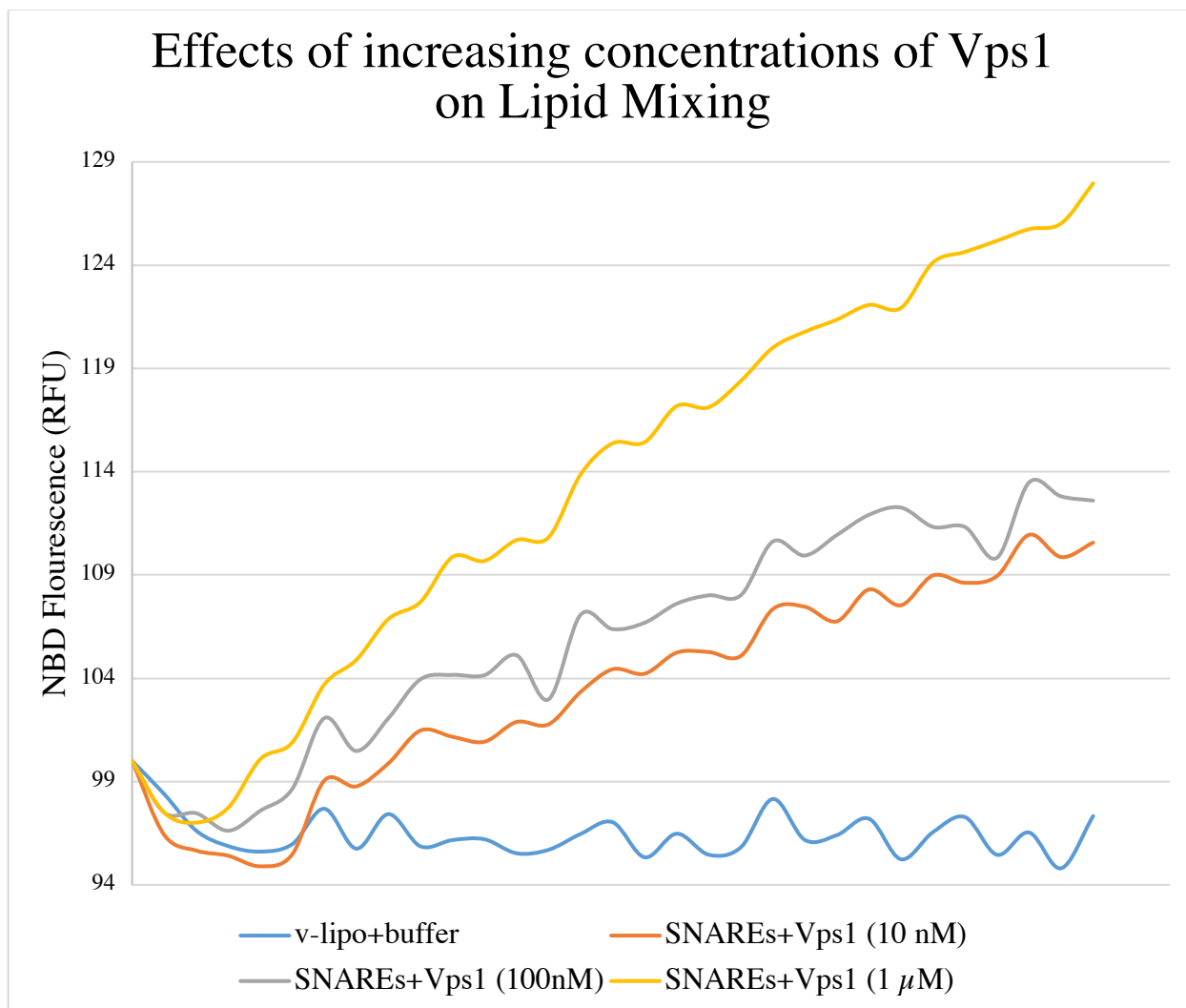
Figure 8: Effects of increasing Vps1 concentration on endosome-to-Golgi fusion. Proteoliposomes for lipid mixing were prepared as described in the methods with the protein concentration used for "Initial Trial Volumes" (Table 3). All wells were prepared with 5 µL *v*-liposomes, 45 µL *t*-liposome, and 10 µM GTP then incubated 2 hours at 4 °C before the addition of Vps1p to start the reaction. Lipid mixing assays were monitored by dequenching of NBD-PE from Liss Rhod-PE (excitation 460nm emission 538 nm) for 2 hours. The increasing concentrations of Vps1 was shown to positively stimulate lipid mixing and 1 µM concentrations were used in all subsequent assays as explained in Results.
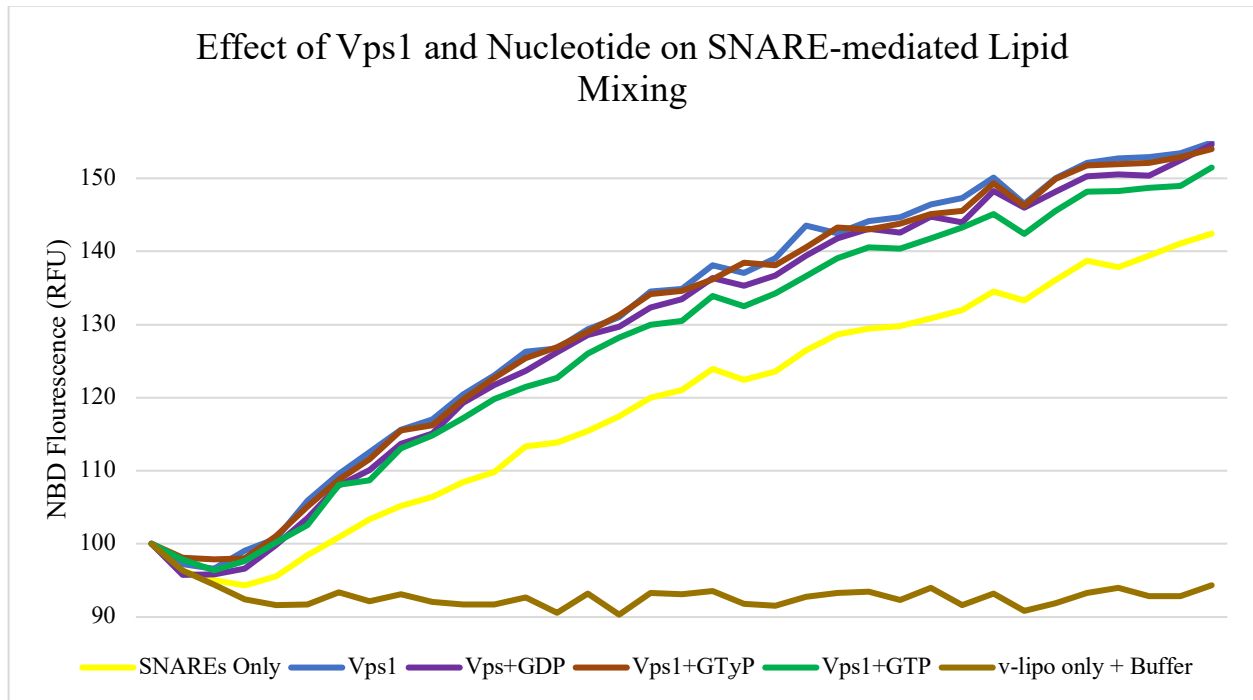
Figure 9a: Effect of Vps1 and nucleotide on assisted lipid mixing. Proteoliposomes for lipid mixing were prepared as described in the methods with the protein concentration used for "Initial Trial Volumes" (Table 3). Control wells were prepared with 5 µL of fluorescent v-liposomes and reconstitution buffer lacking the prepared *t*-liposomes (v-lipo only). All other wells were prepared with 5 µL *v*-liposomes and 45 µL *t*-liposome as in SNAREs only and Vps1 and nucleotide was added to test samples as shown in the figure legend and Table 4. Lipid mixing assays were monitored by dequenching of NBD-PE from Liss Rhod-PE (excitation 460nm emission 538 nm) for 2 hours
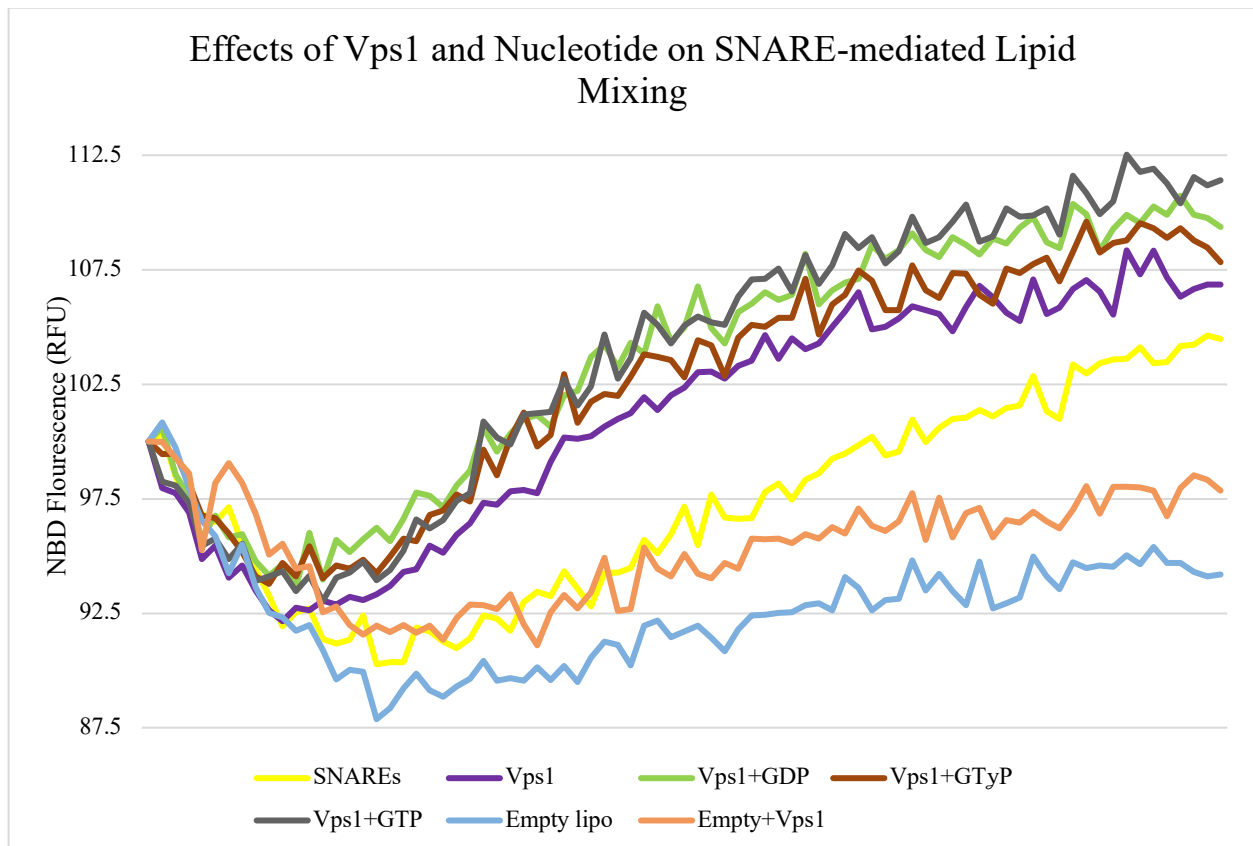
Figure 9b: Effects of Vps1 and nucleotide on assisted lipid mixing. Proteoliposomes for lipid mixing were prepared as described in the methods with the protein concentration used for "Final Assay Volumes" (Table 3). Control wells were prepared with 5 µL of fluorescent *v*-liposomes and 45 µL of *t*-liposomes lacking the incorporated t-SNARE complexes (Empty lipo). All other wells were prepared with 5 µL *v*-liposomes and 45 µL *t*-liposome as in SNAREs only and Vps1 and nucleotide was added to test samples as described in the figure legend and Table 4. Lipid mixing assay monitored by dequenching of NBD-PE from Liss Rhod-PE (excitation 460nm emission 538 nm) for 2 hours
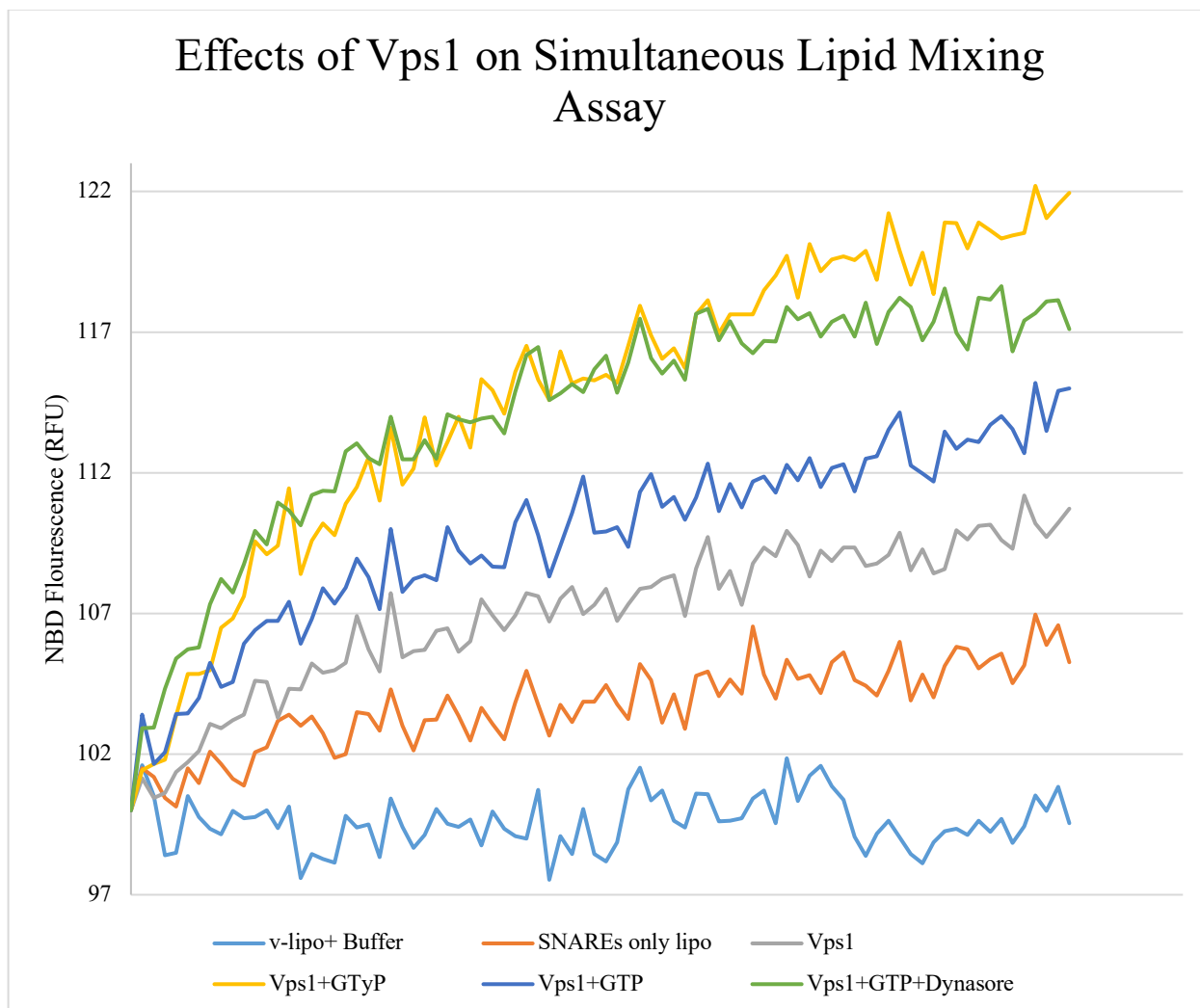
Figure 10a: Simultaneous assay of lipid mixing in the presence of Vps1 and nucleotide. Proteoliposomes for simultaneous lipid mixing were prepared as described in the methods with the protein concentration shown in Table 6 and Table 7. Control wells were prepared with 5 µL of fluorescent *v*-liposomes and 60 µL of reconstitution buffer. All other wells were prepared with 5 µL *v*-liposomes and 45 µL *t*-liposome as in SNAREs only lipo. Vps1 and nucleotide was added to test samples as described in the figure legend and Table 4. Lipid mixing assay monitored by dequenching of NBD-PE from Liss Rhod-PE (excitation 460nm emission 538 nm) for 3 hours
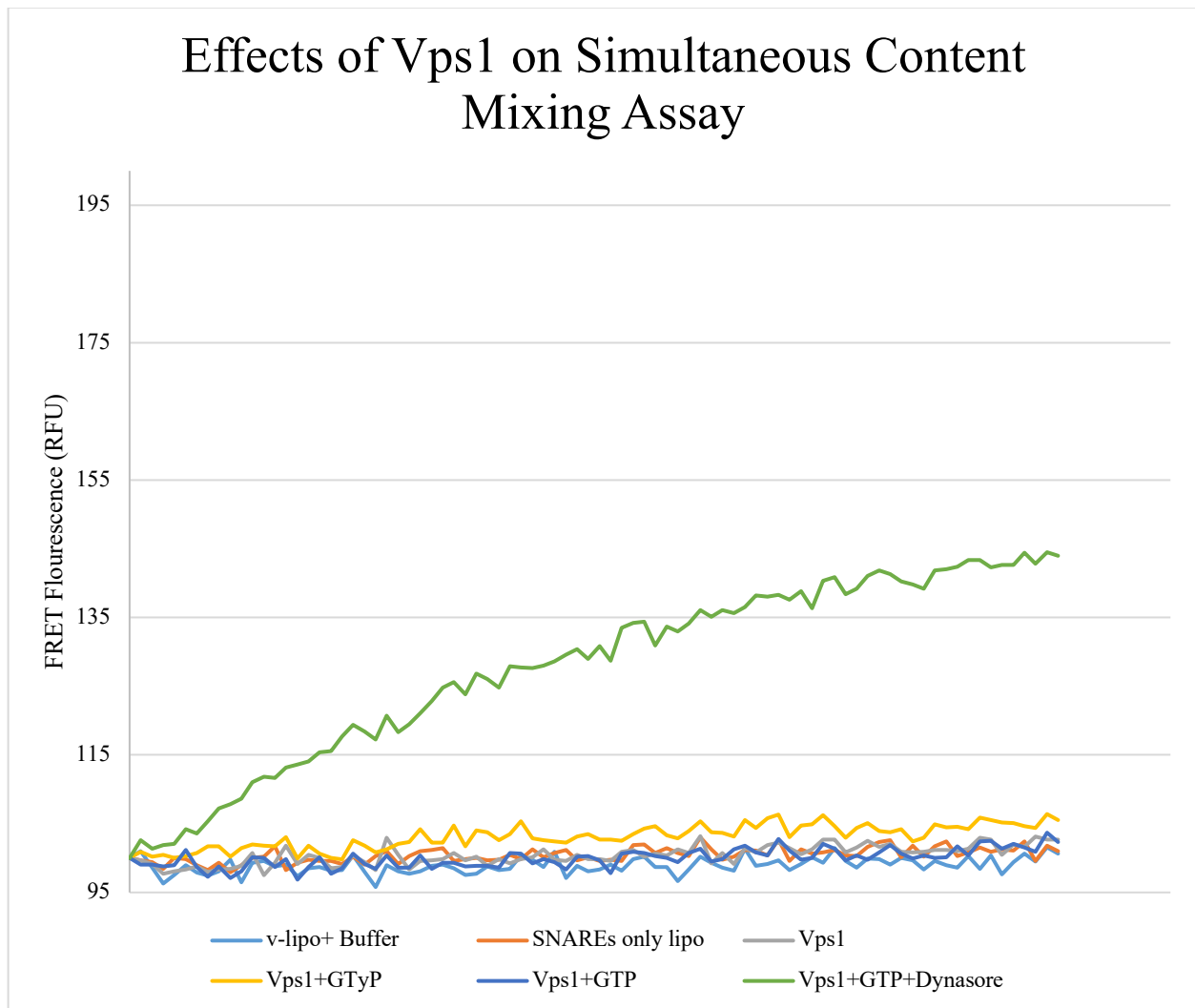
Figure 10b: Simultaneous assay of content mixing in the presence of Vps1 and nucleotide. Proteoliposomes for simultaneous content mixing were prepared as described in the methods with the protein concentration shown in Table 6 and Table 7. Control wells were prepared with 5 µL of fluorescent *v*-liposomes and 60 µL of reconstitution buffer. All other wells were prepared with 5 µL *v*-liposomes and 45 µL *t*-liposome as in SNAREs only lipo. Vps1 and nucleotide was added to test samples as described in the figure legend and Table 4. Content mixing monitored by increased FRET between Cy5-Streptavidin and PhycoE-Biotin (excitation 565 nm, emissions 675 nm) for 3 hours.
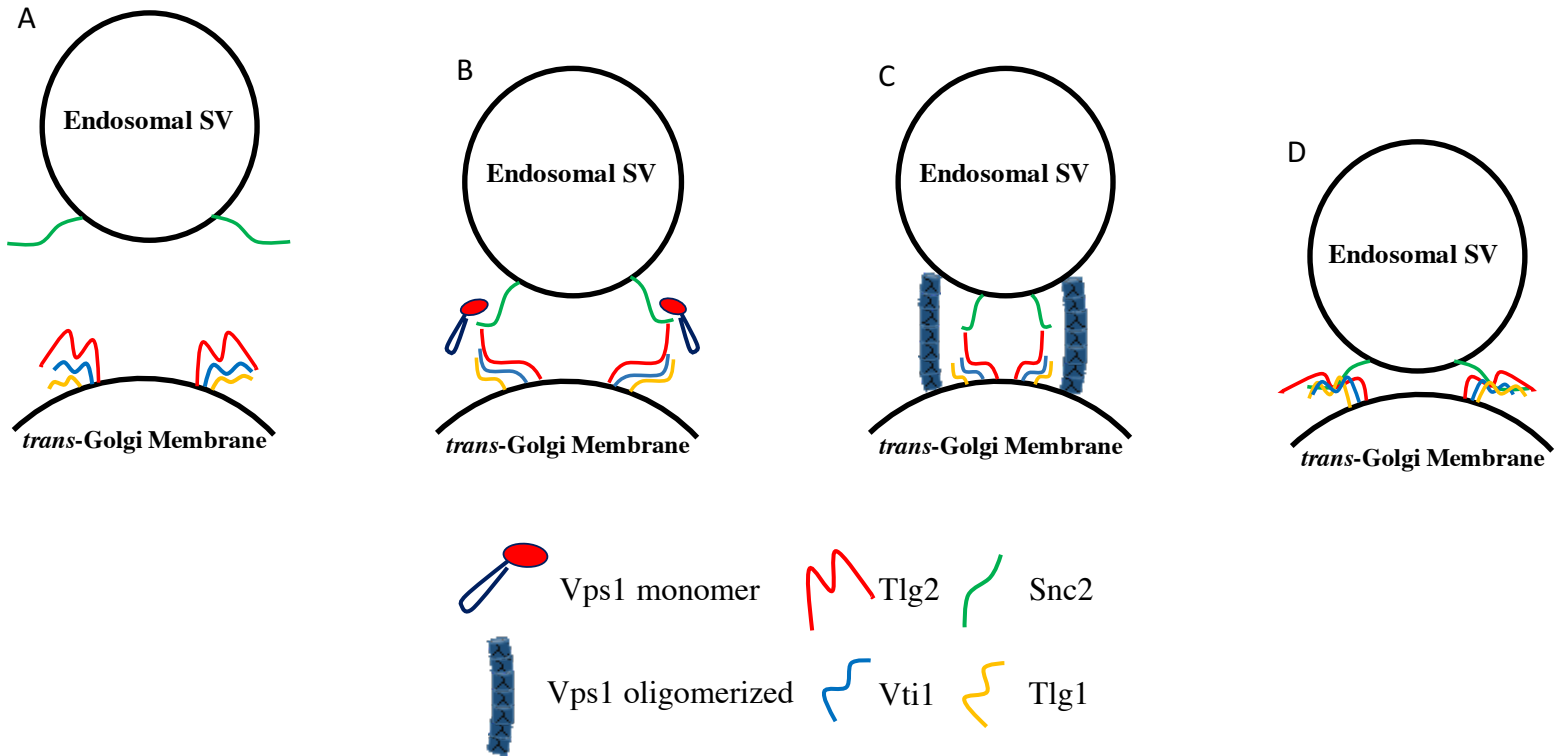
Figure 11: Model of Vps1 stimulated endosome-to-Golgi SNARE-mediated fusion. **A)** Endosome-to-Golgi fusion may require tethering factors, as SNAREs alone do not facilitate significant lipid mixing *in vitro* **B)** Vps1 may facilitate SNARE-mediated fusion by binding *v*-SNARE (Snc2) and *t*-SNARE (Vti1) in the monomer or oligomerized conformation of Vps1 as previous Y2H have shown interaction between Vps1 and both of these SNARE proteins (Makaraci *et al*., 2018). In this sense, Vps1 may act as a bridge between *v*- and *t*-SNAREs to facilitate *trans*-SNARE complex assembly and later fusion. **C)** Conversely, Vps1 may facilitate tethering by directly associating with the liposomal membranes without interacting with the SNARE proteins during *trans*-SNARE assembly. Since the addition of nucleotide was shown to positively enhance fusion, oligomerization of Vps1 may facilitate long range tethering to bring the liposomes into close enough proximity for *trans*-SNARE assembly and eventual zippering and fusion (**D).**